JOSEPHSON JUNCTION CIRCUIT ANALYSIS VIA INTEGRAL MANIFOLDS

by

M. Odyniec and L. O. Chua

Memorandum No. UCB/ERL M82/46

25 March 1982

ELECTRONICS RESEARCH LABORATORY

College of Engineering
University of California, Berkeley
94720

JOSEPHSON JUNCTION CIRCUIT ANALYSIS VIA INTEGRAL MANIFOLDS

M. Odyniec† and L. O. Chua††

ABSTRACT

Using a second-order circuit model the complex dynamical behavior of a typical Josephson-junction circuit is rigorously analyzed using integral manifolds. The key idea is to prove that under certain small-parameter assumptions, the nonautonomous circuit has a stable integral manifold. Moreover this manifold is doubly periodic so that steady state behavior of the Josephson junction circuit reduces to the analysis of its dynamics on a torus. Well-known experimental phenomena, such as the existence of hysteresis in the dc Josephson circuit and voltage steps in the ac Josephson circuit, are rigorously derived and explained

---

Research sponsored by the Air Force of Scientific Research (AFSC) United States Air Force under Contract No. F49620-79-C-0178.

†M. Odyniec is on leave from the Institute of Electronics Fundamentals, Technical University of Warsaw, Poland.

††L. O. Chua is with the Department of Electrical Engineering and Computer Sciences and the Electronics Research Laboratory, University of California, Berkeley, California 94720.

1. Introduction

Josephson junction devices are used in many applications ranging from super-sensitive detectors to superfast computers [13]. This remarkable 2-terminal device is imbued with extremely rich dynamics and displays a wide variety of exotic nonlinear phenomena. For example when driven with dc current source the device is found to oscillate at extremely high frequencies (GHz range). If we plot the average value V_{dc} of the high-frequency voltage versus the dc current I_{dc}, the V_{dc} - I_{dc} characteristic is found to be hysteretic (double-valued). If we connect a sinusoidal current source in parallel with the dc current source and repeat the experiment, the resulting V_{dc} - I_{dc} characteristic changes dramatically. Here discontinuous voltage steps of varying width are observed at rational number multiplies of some natural frequency. This puzzling voltage-step phenomenon had been given various intuitive and physical explanations [13,14]. A rigorous explanation using a first order circuit model (C = 0 in Fig. 1) is given in [1]. Unfortunately this first-order model is over-idealized because it fails to include the effect of junction capacitance C which is always present in non-negligible amounts in the real device.

A more realistic Josephson junction circuit model is shown in Fig. 1 where the basic Josephson element is a nonlinear inductor described by

$$i = I_c \sin(\frac{4\pi e}{h})\phi \qquad (1.1)$$

where ϕ denotes the flux linkage†, e denotes the electron charge and h denotes Planck's constant. The equation governing the second-order circuit in Fig. 1 is given by:

$$C \frac{d^2\phi}{dt^2} + \frac{1}{R}\frac{d\phi}{dt} + I_c \sin(\frac{4\pi e}{h})\phi = I_{dc} + I_{ac} \sin \nu t \qquad (1.2)$$

Equation (1.2) can be transformed into the dimensionless form:††

$$\boxed{\beta\ddot{x} + \dot{x} + \sin x = \alpha + \varepsilon \sin \omega\tau} \qquad (1.3)$$

† The quantity $\frac{4\pi e}{h}\phi$ has an important physical interpretation: it represents the quantum phase difference between the two superconductors which made up the junction.

†† Several autonomous systems (e.g. pendulum with constant torque and viscous damping, synchronous motor, rotating disc, etc.) are described by a similar equation $\frac{d^2x}{dt^2} + a\frac{dx}{dt} + \sin x = b$. Indeed, this equation can be transformed into (1.3) with $\varepsilon = 0$ by defining $\tau := t/a$, $\alpha := b$, and $\beta := a^{-2}$. (Throughout this paper, the symbol := denotes a "definition").

Our objective in this paper is to prove that under certain small-parameter assumptions, solutions of (1.3) are attracted to a doubly-periodic 2-dimensional surface. This surface is called an integral manifold because any trajectory originating from this surface must remain there forever. By identifying appropriate periodic boundaries, this surface can be represented by a torus. Consequently the steady state behavior of (1.3) can be derived by studying the corresponding motion on this torus. This important observation reduces a non-autonomous second-order differential equation on the plane to an equivalent nonautonomous first-order differential equation on the torus. Consequently the same tools as used in [1] (which is applicable only for first-order differential equations) can now be used to analyze (1.3).

In order to prove the existence of an integral manifold for (1.3) it is necessary to analyze the autonomous circuit ($\varepsilon = 0$) first. This is summarized in Section 2 using the analytical method developed by [2]. Unlike the analysis given [1] which was obtained numerically via computer aided phase-plane analysis, the analytical approach here is completely rigorous.

Making use of the result in Section 2, the existence of integral manifold is proved in Section 3.

Although our proof is similar to Hale's [7,9][†] there is a significant difference: Hale's integral manifold arises from closed curve, ours from the curve which is periodic on the plane but is unbounded.

In Section 4 the double periodicity of the unbounded surface derived in Section 3 is used to transform the surface into an equivalent torus. This allows us to apply well-known results from [5,12] to derive the qualitative dynamics of (1.3).

2. D.C. Analysis

In this section we assume that the Josephson junction circuit model in Fig. 1 is driven by a dc current source so that we can set $I_{ac} = 0$ in (1.2), or $\varepsilon = 0$ in (1.3). Defining $y := \dot{x}$, (1.3) transforms into the following autonomous state equation:

$$\dot{x} = y \qquad (2.1a)$$

$$\dot{y} = \frac{\alpha - \sin x - y}{\beta} \qquad (2.1b)$$

[†]Main idea of the proof is due to Krylov-Bogoliubov-Mitropolskii (see [7,9]).

2.1 Qualitative Properties

The qualitative properties of (2.1) can be derived by physical reasoning [10,13,14], computer-aided phase-plane analysis [1,6], or by a more rigorous analytic approach [2,8].

In this section we summarize and interpret geometrically the qualitative properties derived in [2,8]. This geometrical interpretation will play a crucial role in our ac analysis in Sections 3 and 4.

Since the right-hand side of (2.1) is 2π-periodic in x, the phase portrait will duplicate itself every 2π intervals. Hence, it suffices to consider only a vertical strip of width 2π, say $\{(x,y) : 0 \leq x < 2\pi, y \in R\}$, instead of the entire x-y plane. A rigorous analysis of the phase portrait of (2.1) in this vertical strip can be found in [2,8]. Outline of Andronov's approach and additional details are given in Appendix A. In particular, it can be shown that for $\beta := RC\Omega > 0$ the phase portrait of (2.1) can exhibit only 7 qualitatively distinct behaviors, as depicted in Figs. 2(a)-(g) depending on the value of $\alpha := I_{dc}/I_c$.

For simplicity, we assume $\alpha \geq 0$ in summarizing the following qualitative properties. The same properties hold, *mutatis mutandis*, for $\alpha \leq 0$.

Case 1. $\alpha > 1$, $\beta > 0$ (Fig. 2(a))

System (2.1a) has a unique 2π-periodic† and globally stable trajectory $y = \psi(x)$, $\psi(x) > 0$, which attracts all other trajectories. There are no equilibrium points. See Fig. 2(a)

Case 2. $0 < \alpha \leq 1$, $\beta > \beta_0(\alpha)$ (Figs. 2(b) and (c))

For any $\alpha \in (0,1]$ there is a critical value $\beta_0 = \beta_0(\alpha)$ such that for $\beta > \beta_0(\alpha)$, system (2.1) has a unique 2π-periodic asymptotically-stable trajectory $y = \psi(x)$, $\psi(x) > 0$, which attracts all trajectories outside the domain of attraction of equilibrium points.

For $\alpha = 1$, the equilibrium points are located at $(x,y) = (\frac{\pi}{2} + k2\pi, 0)$, $k = 0, \pm1, \pm2, \ldots$ (Fig. 2(b)). For $0 < \alpha < 1$, the equilibrium points located at $(x,y) = (\sin^{-1} \alpha, 0)$ are either stable nodes or stable foci. Those located

†Throughout this section, the 2π-periodicity is with respect to x. This implies that y(t) is also periodic with respect to time (with period $T = \int_0^{2\pi} \frac{dx}{\psi(x)}$). See Corollary 4.

at $(x,y) = (\pi - \sin^{-1}\alpha, 0)$ are saddle points (Fig. 2(c)).

Case 3 $\quad 0 < \alpha \leq 1,\ 0 < \beta \leq \beta_0(\alpha)$ (Figs. 2(d)-(g))

System (2.1) has no periodic solution.† For $\beta < \beta_0(\alpha)$ (Figs. 2(f) and (g)), the trajectories tend, either (for $\alpha = 1$) toward the unstable points located at $(x,y) = (\frac{\pi}{2} + k2\pi, 0)$ or (for $0 < \alpha < 1$) toward stable equilibria at $(x,y) = (\sin^{-1}\alpha + 2k\pi, 0)$ (except for a pair of trajectories converging toward each saddle). For $\beta = \beta_0(\alpha)$ (Figs. 2(d) and (e)), the trajectories connecting unstable points form a separatrix. Trajectories originating above the separatrix tend toward it. Trajectories originating below it behave as in the case $\beta < \beta_0(\alpha)$.

It can be shown that the "critical value" $\beta_0 = \beta_0(\alpha)$ is a continuous and one-to-one function of α over the interval $0 < \alpha \leq 1$ [8]. Since $\beta := R^2C\frac{4\pi e}{h}I_c$ depends only on device parameters and is therefore fixed for a given Josephson junction, it is more natural to refer to the inverse function $\alpha = \alpha_0(\beta)$ which is defined over the interval $\beta_0(1) \leq \beta < \infty$ (Fig. 3(a)). Since the phase portrait in Fig. 2(f) includes the range $\beta < \beta_0(1)$ when $\alpha = 1$, let us extend the domain of $\alpha = \alpha_0(\beta)$ over the interval $0 < \beta < \infty$ by defining $\alpha_0(\beta) = 1$ for $0 < \beta \leq \beta_0(1)$. This extended function is shown in Fig. 3(a) for future reference.

Comparing Figs. 2 and 3(a) we note that for each fixed $\beta = \hat{\beta}$, we can read off the critical value $\alpha_0(\hat{\beta})$ such that (2.1) has a 2π-periodic trajectory $y = \psi(x)$ if $\alpha > \alpha_0(\hat{\beta})$, and no such trajectory if $\alpha < \alpha_0(\hat{\beta})$ †† The phase portrait for the special case $\alpha = \alpha_0(\hat{\beta})$ is given by Fig. 2(d) if $\hat{\beta} = \beta_0(1)$, Fig. 2(e) if $\hat{\beta} > \beta_0(1)$, and Fig. 2(f) if $\hat{\beta} < \beta_0(1)$.†††

The following properties of the critical function $\alpha_0(\beta)$ are proved in Appendix A:

Property 1 (See Fig. 3(a)).

$\alpha = \alpha_0(\beta)$ is a continuous function defined for $\beta > 0$ and satisfying:

---

†In this case, except for constant solutions corresponding to equilibrium points, $y(\tau)$ is not a periodic function of time.

††To see this fix $\beta = \hat{\beta}$ in Fig. 3(a) and observe that for any $\alpha > \alpha_0(\hat{\beta})$ the corresponding critical value $\beta_0(\alpha)$ is less than $\hat{\beta}$. Since $\hat{\beta} > \beta_0(\alpha)$ corresponds to Figs. 2(b) and (c) and hence has a 2π-periodic trajectory $\psi(x)$.

†††In terms of $\alpha_0(\beta)$ Figs. 2(b)-(g) correspond to:

(b) $\alpha_0(\beta) < \alpha = 1$ (c) $\alpha_0(\beta) < \alpha < 1$

(d) $\alpha = \alpha_0(\beta) = 1,\ \beta = \beta_0(1)$ (e) $\alpha = \alpha_0(\beta) < 1 \quad \beta > \beta_0(1)$

(f) $\alpha = \alpha_0(\beta),\ \beta < \beta_0(1)$ (g) $0 < \alpha < \alpha_0(\beta)$ (see Fig. 3a)

(a) $\alpha_0(\beta) = 1$, for $0 < \beta \leq \beta_0(1)$,

(b) for $\beta > \beta_0(1)$, $\alpha_0(\beta)$ is strictly decreasing,

(c) $\lim\limits_{\beta \to +\infty} a_0(\beta) = 0$

Property 2.

Let $\psi(x) = \psi_{\alpha\beta}(x)$ denote the 2π-periodic trajectory corresponding to a specific parameter values α and β.

(a) For any $\beta_1 > \beta_2 > 0$ and any $\alpha > \alpha_0(\beta_2)$, we have†:

$$\psi_{\alpha\beta_1}(x) > \psi_{\alpha\beta_2}(x), \text{ for any } x.$$

(b) For any $\beta_0 > 0$ and any $\alpha_1 > \alpha_2 > \alpha_0(\beta_0)$, we have:

$$\psi_{\alpha_1\beta}(x) > \psi_{\alpha_2\beta}(x), \text{ for any } x.$$

2.2 Geometrical Interpretation

In the τ-x-y space, the 2π-periodic trajectory $y = \psi(x)$ of (2.1) can be interpreted as a periodic surface

$$S_0 := \{(\tau,x,y) \in R^3 : y = \psi(x),\ \tau \in R,\ x \in R\}$$

as shown in Fig. 4(a). The surface S_0 is invariant in the sense that any trajectory (in τ-x-y space) starting from a point (τ_0,x_0,y_0) on S_0 at $\tau = \tau_0$ remains on S_0 for all $\tau \geq \tau_0$ (and $\tau < \tau_0$). S_0 is called an integral manifold of (2.1), a concept of fundamental importance in this paper [7,9].

Since both S_0 and the right-hand-side of (2.1) are 2π-periodic in x, we can "chop" S_0 into parallel strips $\{(\tau,x,y) \in S_0 : 2k\pi \leq x < 2(k+1)\pi\}$, $k = 0, \pm1, \pm2, \ldots$ and consider all lines $x = 2k\pi$, $k = 0, \pm1, \pm2, \ldots$ as identical.

If we wrap S_0 around so that these lines coincide, we would obtain the cylinder shown in Fig. 4(b).

Since (2.1) is autonomous the cross sections of Figs. 4(a) and (b) taken at times $\tau = kT_1$, $k = 0, \pm1, \pm2, \ldots$ for arbitrary T, are all identical. Consequently, we can identify these cross-sections and transform the cylinder in Fig. 4(b) into the torus in Fig. 4(c).

Hence, the integral manifold S_0 of (2.1) can be represented geometrically by Fig. 4(a), (b) or (c).

†Recall that the 2π-periodic solution $\psi_{\alpha\beta}$ does not exist for $\alpha \leq \alpha_0(\beta)$.

It follows from the stability property of $\psi(x)$ (See Figs. 2(a), (b), and (c)), that for $\alpha > 1$, S_0 attracts all trajectories outside of S_0; for $\alpha_0 < \alpha < 1$ trajectories outside of S_0 are attracted to either S_0 or to stable constant solutions of (2.1). Hence, every nonconstant periodic solution of (2.1) must lie on the integral manifold S_0.

Given the periodic (in x) trajectory $y = \psi(x)$ we can determine the corresponding solution waveform $x^*(\tau) := x^*(\tau;\tau_0,x_0)$ by solving the scalar initial value problem

$$\dot{x} = \psi(x), \ x(\tau_0) = x_0 \tag{2.2}$$

derived from (2.1a). Once $x^*(\tau)$ is found, we can determine $y^*(\tau) = \psi[x^*(\tau)]$ by direct substitution. Note that every solution $(x^*(t), y^*(t))$ obtained from (2.2) lies on the integral manifold S_0, and vice-versa. Hence, if we are interested only in the nonconstant periodic solutions of (2.1), it suffices to study solutions on the integral manifold S_0. The transformation from a 2-dimensional problem (2.1) into a 1-dimensional problem (2.2) is in fact the main motivation for introducing the integral manifold S_0.

Of course $\psi(x)$ is seldom available in analytic form. However, we will now demonstrate that many significant qualitative information concerning (2.1) can be obtained from the qualitative properties of $\psi(x)$.

Property 3.

For any initial condition x_0, the solution of (2.2) is of the form

$$x(\tau) = \frac{2\pi}{T}\tau + p(\tau) \tag{2.3}$$

where $T := \int_0^{2\pi} \frac{dx}{\psi(x)}$ and $p(\tau)$ is T-periodic.

Proof: This is a simple consequence of the 2π-periodicity and positiveness of $\psi(x)$. For details see [12]. ¤

Corollary 4.

For any initial condition taken on the integral manifold S_0, (2.1) has a T-periodic solution† $(x(\tau),y(\tau))$ where $x(\tau)$ is of the form (2.3) and $y(\tau) = \psi[x(\tau)]$.

Proof: Follows directly from the definition of S_0. ¤

†$(x(\tau),y(\tau))$ is T-periodic on the cylinder in Fig. 4(b).

Corollary 5

The period T depends on α and β ($\alpha > \alpha_0$, $\beta > 0$) and decreases when either α or β increases.

Proof: Follows directly from Properties 1 and 2 and $T := \int_0^{2\pi} \frac{dx}{\psi(x)}$. ¤

Corollary 6

1. For any $\alpha > 0$, $T \geq \frac{2\pi}{\alpha+1}$

2. For any $\alpha > 1$, $T \leq \frac{2\pi}{\alpha-1}$

Proof: It follows from (2.1) that

$$\frac{d\psi}{dx} = \frac{\dot{\psi}[x(\tau)]}{\dot{x}} = \frac{\alpha - \sin x - y}{\psi(x)} = 0$$

only on the line $y = \alpha - \sin x$. Since $\psi(x)$ is differentiable, its global maximum and mimimum must lie on $y = \alpha - \sin x$. So $\alpha - 1 \leq \psi(x) \leq \alpha + 1$ and $\frac{2\pi}{\alpha+1} \leq T = \int_0^{2\pi} \frac{dx}{\psi(x)} \leq \frac{2\pi}{\alpha-1}$. ¤

Another important property of an "integral manifold" is that its qualitative properties are often preserved under small perturbations. In the following Section 3, we will demonstrate this property by showing that if the right hand side of (2.1) is perturbed slightly, then the resulting equation would still possess an integral manifold S_ε which is "near" to S_0. Moreover the qualitative properties of solutions on S_ε can be derived by analyzing an associated scalar first-order differential equation.

2.3 Physical Interpretation

We will now relate the preceding qualitative properties and geometrical interpretations in terms of the physical behavior of the Josephson-junction circuit model in Fig. 1 when driven by a dc current source.

Recall that since x is proportional to the magnetic flux (i.e. phase difference) $y = \dot{x}$ can be interpreted as a "normalized" terminal voltage corresponding to the "normalized" dc input current $\alpha := I_{dc}/I_c$.

The following physical interpretation then follows directly:

1. So long as the dc input current is smaller than the maximal admissible supercurrent I_c ($I_{dc} \leq I_c$ or $\alpha \leq 1$), there exists a constant (in time) phase-difference $\phi := \sin^{-1}(I_{dc}/I_c)$ across the junction. Hence v = 0, i.e., the voltage drop is zero and the junction functions as a superconductor.

2. For any choice of the parameter[†] $\beta := RC\Omega = R^2 C I_c \frac{4\pi e}{h}$, there exists a critical input current $I_0 := \alpha_0 I_c$ (See Fig. 3(b)) such that for $I_{dc} > I_0$ (i.e. $\alpha > \alpha_0$), the phase-difference across the junction assumes the time-varying form:[††]

$$\phi(t) := x(\Omega t) = \frac{2\pi}{T} \Omega t + p(\Omega t)$$

The associated terminal voltage is therefore time-varying and assumes the form[†††]:

$$v(t) = RI_c \psi[\frac{2\pi}{T} \Omega t + p(\Omega t)]$$

where $\psi(x)$ is a T-periodic function. In other words, the period of the terminal voltage is equal to T/Ω (where T is a dimensionless constant given in Property 3).

3. Since Ω is a very large number for Josephson junction devices, the oscillation frequency is extremely high (in the GHz range). Consequently, only the average voltage:

$$V_{dc} := \frac{\Omega}{T}\int_0^{\frac{T}{\Omega}} v(t)dt = \frac{\Omega}{T}\frac{h}{4\pi e}\int_0^{\frac{T}{\Omega}} \frac{d\phi(t)}{dt}\, dt = \frac{RI_c}{T}\, \phi(t)\Big|_0^{\frac{T}{\Omega}} = \frac{RI_c}{T} \cdot 2\pi = \frac{h}{2e}\frac{\Omega}{T}$$

can be measured experimentally. This average or dc voltage is therefore proportional to the oscillation frequency $\frac{\Omega}{T}$.

4. It follows from Corollary 5 that the dc voltage V_{dc} increases with I_{dc} and C ($\beta = RC\Omega$) when $R\Omega = R^2 I_c \frac{4\pi e}{h}$ is held constant.

Since a constant I_{dc} and β result in a constant T, whereas Ω increases with R, it follows that the dc voltage V_{dc} will increase with R when $\beta = R^2 C \frac{4\pi e}{h} I_c$ is held constant.

5. For $I_0 < I_{dc} \leq I_c$ (i.e. $\alpha_0 < \alpha \leq 1$) both constant and oscillatory steady states coexist. Therefore the $V_{dc} - I_{dc}$ characteristic will be a double-valued function in this interval. This observation has been verified

---

[†]Recall that for $\beta \leq \beta_0(1)$, $\alpha_0 = 1$. Compare Fig. 3(b) and the discussion in case 2.

[††]Note that time $\tau := \Omega t$ and period T are dimensionless while frequency Ω and time t are physical quantities.

[†††]
$$v(t) = \frac{h}{4\pi e}\frac{d\phi(t)}{dt} = \frac{h}{4\pi e}\frac{dx(\Omega t)}{dt} = \frac{h}{4\pi e}\Omega\dot{x}(\Omega t) = \frac{h}{4\pi e}\Omega\psi[x(\Omega t)]$$
$$= RI_c\psi[\frac{2\pi}{T}\Omega t + p(\Omega t)]$$

experimentally [10,13,14] and is reproduced in Fig. 5. Note that for junction capacitance C sufficiently small (i.e. $\beta \leq \beta_0(1)$), we have $I_0 = I_v$ ($\alpha_0 = 1$) and the $V_{dc} - I_{dc}$ characteristic becomes a single-valued function. See Figs. 3 and 5.

6. It follows directly from Property 2 and the phase protrait discussion, that the critical current I_0 is a monotonically-decreasing function of the junction capacitance C, as shown in Fig. 3. Detailed proof of this relationship was given in [8] see also Appendix A. The quantitive relationship has been derived numerically in [1,8] and experimentally in [10].

3. AC Analysis: Existence of Integral Manifold.

3.1 Introduction

Consider now (1.3) which applies when the Josephson junction circuit model is driven by a sinusoidal current source with normalized amplitude $\varepsilon := I_{ac}/I_c$. Defining $y := \dot{x}$, we obtain the following non-autonomous state equations:

$$\dot{x} = y \tag{3.1a}$$

$$\dot{y} = \frac{\alpha - \sin x - y + \varepsilon \sin \omega\tau}{\beta} \tag{3.1b}$$

In general we cannot expect the solutions of (3.1) to remain close to those of the autonomous system (2.1) over the infinite time interval, even for small ε. However, we will show in this section that (3.1) has an integral manifold provided the parameters β and ε lie within the shaded region in Fig. 6(a) when $\alpha \leq 1$ or Fig. 6(b) when $\alpha > 1$. Moreover, for ε sufficiently small, we will show that the integral manifold S_ε of (3.1) is close to the integral manifold S_0 of the autonomous system (2.1), while for β sufficiently small the integral manifold S_β is close to the surface

$$\{(\tau,x,y) : y = \alpha - \sin x + \varepsilon \sin \omega\tau,\ x \in \mathbb{R},\ \tau \in R\}.$$

Just as in Section 2 the existence of an integral manifold for (3.1) will allow us to derive a number of important qualitative properties of (3.1) in Section 4 by studying an associated first order differential equation. This order-reduction possibility is in fact our main motivation for finding integral manifolds.

3.2. Integral manifold S_ε associated with small ε.

Recall the integral manifold

$$S_0 := \{(\tau,x,y) \in R^3 : y = \psi(x),\ x \in R,\ \tau \in R\} \tag{3.2}$$

of the autonomous system (2.1), where $y = \psi(x)$ is the 2π-periodic (in x) trajectory depicted in Fig. 2. Since our objective in this section is to show the existence of an integral manifold S_ε of (3.1) which is close to S_0, it is convenient to introduce a new coordinate system (θ,ρ) defined as follows:

$$x := \theta - \psi'(\theta')\rho \tag{3.3a}$$

$$y := \psi(\theta) + \rho \tag{3.3b}$$

To obtain geometrical interpretation of (3.3), note that when $\rho = 0$ we obtain $x = \theta$ and $y = \psi(\theta)$, which is simply a parametric equation describing $y = \psi(x)$. For (x,y) sufficiently close to $y = \psi(x)$ it can be shown [7] that the coordinate transformation (3.3) is one-to-one. Hence, to each point $P_0 = (x_0,y_0)$ near $y = \psi(x)$, there correspond a unique pair (θ_0,ρ_0).

Let us project any point $P_0 = (x_0,y_0)$ near $y = \psi(x)$ "orthogonally" onto the trajectory as shown in Fig. 7. Define θ_0 so that the point of intersection $\hat{P}_0$ has coordinates $\hat{x}_0 = \theta_0$, $\hat{y}_0 = \psi(\theta)$.

Observe that the vectors $[1,\psi'(\theta_0)]$ and $[-\psi'(\theta_0),1]$ are just the tangent and orthogonal vectors to the trajectory at the point $\hat{P}_0 = (\hat{x}_0,\hat{y}_0)$. Observe next that $y_0 - \hat{y}_0 = -\frac{1}{\psi'(\theta_0)}(x_0 - \hat{x}_0)$. Hence, if we define $\rho_0 := y_0 - y_0$ we get formulas (3.3):

$$x_0 = \hat{x}_0 + \psi'(\theta_0)\rho_0 = \theta_0 - \psi'(\theta_0)\rho_0$$

$$y_0 = \hat{y}_0 + \rho_0 = \psi(\theta_0) + \rho_0$$

i.e. coordinates θ_0, ρ_0 correspond to the point P_0. In terms of the new coordinates θ and ρ (3.1) becomes (see Appendix B):

$$\dot{\theta} = \psi(\theta) + G(\tau,\theta,\rho,\varepsilon) \tag{3.4a}$$

$$\dot{\rho} = A(\theta)\rho + F(\tau,\theta,\rho,\varepsilon) \tag{3.4b}$$

The following basic theorem shows that for ε sufficiently small and for appropriately chosen initial conditions, (3.4) can be reduced to one scalar equation.

Theorem 3.1 [11]

If (2.1) has an integral manifold S_0 as defined in (3.2) then for ε sufficiently small, (3.1) has a stable integral manifold

$$S_\varepsilon := \{(\tau,x,y) \in \mathbb{R}^3 : x = \theta - \psi'(\theta)h(\tau,\theta,\varepsilon),\ y = \psi(\theta) + h(\tau,\theta,\varepsilon),\ \theta \in \mathbb{R},\ \tau \in \mathbb{R}\} \tag{3.5}$$

where the function $h(\cdot,\cdot,\cdot)$ satisfies the following properties:

(a) $h(\tau,\theta,\varepsilon)$ is smooth† and bounded by D_ε where $\lim_{\varepsilon\to 0} D_\varepsilon = 0$.

(b) $h(\tau,\theta,\varepsilon)$ is Lipschitzian in θ with Lipschitz constant Δ_ε, where $\lim_{\varepsilon\to 0} \Delta_\varepsilon = 0$.

(c) $h(\tau,\theta,\varepsilon)$ is 2π-periodic in θ and $\frac{2\pi}{\omega}$-periodic in τ.

Moreover, for any initial condition on S_ε, i.e. for any $(\tau_0,x(\tau_0),y(\tau_0)) \in S_\varepsilon$, the solution of (3.1) has the following form:

$$x(\tau) = \theta(\tau) + \psi'(\theta(\tau))h(\tau,\theta(\tau),\varepsilon) \tag{3.6a}$$

$$y(\tau) = \psi(\theta(\tau)) + h(\tau,\theta(\tau),\varepsilon) \tag{3.6b}$$

where $\theta(\tau)$ is a solution (with initial condition $\theta(\tau_0) = \theta_0$) of the scalar equation:

$$\dot{\theta} = \psi(\theta) + \bar{G}(\tau,\theta,\varepsilon) \tag{3.7}$$

where $\bar{G}(\tau,\theta,\varepsilon) := G(\tau,\theta,h(\tau,\theta,\varepsilon),\varepsilon)$ is $\frac{2\pi}{\omega}$-periodic in τ, 2π-periodic in θ and tends to zero with ε.

Remarks: 1. Geometrically speaking Theorem 3.1 asserts that under small perturbation the surface S_0 will not change much. In particular, since $h(\tau,\theta,\varepsilon) \to 0$ (uniformly) as $\varepsilon \to 0$ it follows that S_ε tends to S_0 as $\varepsilon \to 0$.

2. Since the proof of Theorem 3.1 is very long we will give only main steps here, with additional details given in Appendix C.

Outline of the proof of Theorem 3.1:

The basic idea of the proof consists of defining a "family of candidates for integral manifold" together with appropriate transformation which maps this family into itself. Let $H(\tau,\theta,\varepsilon)$ be such a "candidate".

---

†For our purposes it is enough to require that $h(\tau,\theta,\varepsilon)$ has continuously differentiable derivatives up to the order 4, with respect to τ and θ.

Let $\theta^H(\tau) = \theta^H(\tau;\tau_0,\theta_0)$ denote the solution of the <u>scalar</u> equation

$$\dot{\theta} = \psi(\theta) + G(\tau,\theta,H(\tau,\theta,\varepsilon),\varepsilon) \tag{3.8}$$

with initial condition $\theta(\tau_0) = \theta_0$ (i.e. solution of (3.4a) with $\rho(t)$ replaced by $H(\tau,\theta,\varepsilon)$).

Consider next the linear part of (3.4b)

$$\dot{\rho} = A(\theta^H(\tau))\rho \tag{3.9}$$

Let $\gamma(\tau,\tau_0)$ denote the fundamental solution of (3.9), i.e.,

$$\gamma(\tau,\tau_0) := \exp\left[\int_{\tau_0}^{\tau} A(\theta^H(t))dt\right] \tag{3.10}$$

For any $H(\tau,\theta,\varepsilon)$ define the transformation T[†] as follows:

$$T[H](\tau_0,\theta_0) := \int_{-\infty}^{0} \gamma(s+\tau_0,\tau_0) \cdot F[s+\tau_0,\theta^H(s+\tau_0;\tau_0,\theta_0), H(s+\tau_0,\theta^H(s+\tau_0;\tau_0,\theta_0,\varepsilon),\varepsilon)]ds \tag{3.11}$$

Assume that all candidates for integral manifold satisfy hypotheses (a), (b) and (c) and denote the space of all candidates by $C(D_\varepsilon,\Delta_\varepsilon)$. Our next task is to show that for ε sufficiently small the transformation T maps $C(D_\varepsilon,\Delta_\varepsilon)$ into itself and is a contraction. It then follows that the sequence of successive iterates $H_n = T H_{n-1}$, $n \in 1,2,3,\ldots$, $H_0 \in C(D_\varepsilon,\Delta_\varepsilon)$, converges to the unique fixed point h of T i.e. $h = Th$. It follows from the definition of T and h that $h(\tau,\theta,\varepsilon)$ constitutes an integral manifold for (3.4) and that for any θ_0,τ_0 and $\rho(\tau_0) = \rho_0 = h(\tau_0,\theta_0)$, (3.4) is equivalent to:

$$\dot{\theta} = \psi(\theta) + G[\tau,\theta,h(\tau,\theta,\varepsilon),\varepsilon] \tag{3.12a}$$

$$\rho(\tau) = h(\tau,\theta,\varepsilon) \tag{3.12b}$$

It is natural to ask how the transformation T was found. The following remarks provide some intuitive explanation (in the case when A is constant see also p. 235 of [7]). Suppose that (3.4) has an integral manifold S_ε in the (τ,θ,ρ)-space and suppose ρ can be expressed as a function of θ; namely

---

[†] Intuitive explanation on how the form of T was obtained is given at the end of the outline. See also [7].

$\rho = h(\tau,\theta,\varepsilon)$. If we choose initial condition as $\tau_0, \theta_0, \rho_0 = h(\tau_0,\theta_0,\varepsilon)$, then (3.4) is equivalent to:

$$\dot{\theta} = \psi(\theta) + G(\tau,\theta,h(\tau,\theta,\varepsilon),\varepsilon) \tag{3.13a}$$

$$\frac{d}{d\tau} h(\tau,\theta(\tau),\varepsilon) = A(\theta)h(\tau,\theta,\varepsilon) + F(\tau,\theta,h(\tau,\theta,\varepsilon),\varepsilon) \tag{3.13b}$$

for any τ_0, θ_0. Let $\theta^h(\tau) = \theta^h(\tau;\tau_0,\theta_0)$ denote the solution of (3.13a). Viewing (3.13b) as a linear equation with a forcing function $\varepsilon F(\cdot,\cdot,\cdot,\cdot)$, we can write the equation in the integral form:

$$h(\tau,\theta^h(\tau),\varepsilon) = \gamma(\tau,\tau_0)h(\tau_0,\theta_0,\varepsilon) + \int_{\tau_0}^{\tau} \gamma(\tau,s)F(s,\theta^h,h(s,\theta^h,\varepsilon),\varepsilon)ds \tag{3.14†}$$

where $\gamma(\tau,\tau_0)$ is defined by (3.10). Multiplying both sides of (3.14) by $\gamma(\tau_0,\tau)$ we obtain:

$$\gamma(\tau_0,\tau)h(\tau,\theta^h,\varepsilon) = h(\tau_0,\theta_0,\varepsilon) + \int_{\tau_0}^{\tau} \gamma(\tau_0,s)F(s,\theta^h,h(s,\theta^h,\varepsilon),\varepsilon)ds.$$

Assuming that $\gamma(\tau_0,\tau) \to 0$ as $\tau \to -\infty$, which holds if $\int_0^{2\pi} A(\theta)d\theta < 0$, we have $\gamma(\tau_0,\tau)h(\tau,\theta^h,\varepsilon) \to 0$ as $\tau \to -\infty$ because $h(\tau,\theta^h,\varepsilon)$ must be bounded. Hence

$$h(\tau_0,\theta_0,\varepsilon) = -\int_{\tau_0}^{-\infty} \gamma(\tau_0,s)F(s,\theta^h,h(s,\theta^h,h(s,\theta^h,\varepsilon),\varepsilon)ds.$$

Changing the dummy variable s to $\sigma := s - \tau_0$ we obtain

$$h(\tau_0,\theta_0,\varepsilon) = \int_{-\infty}^{0} \gamma(\tau_0,\tau_0+\sigma)F(\tau_0+\sigma,\theta^h(\tau_0+\sigma;\tau_0,\theta_0), h(\tau_0+\sigma,\theta^h(\tau_0+\sigma;\tau_0,\theta_0),\varepsilon)d\sigma$$

which is precisely (3.11). ⌑

<u>Theorem 3.1</u> asserts that for ε sufficiently small, (3.1) has an <u>integral manifold</u> consisting of a <u>periodic surface</u> S_ε which is close to the integral manifold S_0 of (2.1) as shown in Fig. 8(a). Cross sections of S_0 at any time are identical and described by $y = \psi(x)$. For comparison purposes the curve $y = \alpha - \sin x$ ($\tau = 0$) for $\alpha > 1$ is also shown to emphasize that it need not be close to $y = \psi(x)$.

---

† θ^h denotes here $\theta^h(s) = \theta^h(s;\tau_0,\theta_0)$.

In Section 4, we will show that (3.1) has a periodic solution which lies on S_ε. This periodic solution however need not be close to the periodic solution of (2.1) even if S_ε is close to S_0. Before proceding further let us note that for $\alpha \in [0,1)$ (3.1) possess stable periodic solutions which lie outside of S_ε. More exactly we have:

Theorem 3.2 [4,7]

If $\alpha \in (0,1)$ and ε is sufficiently small then there exist:

(a) a unique (in $x \in (0,2\pi]$ strip) asymptotically stable $\frac{2\pi}{\omega}$ -periodic solution of (3.1) in a neighborhood of the stable equilibrium point $(\sin^{-1}\alpha,0)$ of (2.1). Moreover this solution tends to the stable constant (equilibrium) solutions as $\varepsilon \to 0$.

(b) a unique (in $x \in (0,2\pi]$ strip) unstable $\frac{2\pi}{\omega}$ -periodic solution of (3.1) in a neighborhood of the unstable equilibrium point $(\pi - \sin^{-1}\alpha,0)$ of (2.1). Moreover this solution tends to the unstable constant (equilibrium) solution as $\varepsilon \to 0$.

Proof: In a neighborhood of an equilibrium point, equations (3.1) can be reduced to $\dot{\rho} = A\rho + F(\tau,\rho,\varepsilon)$ which is (3.4) with θ absent and $\rho \in \mathbb{R}$. The proof then goes along the lines of the one of Theorem 3.1 [7]. ¤

Remarks:

1. The constant solutions (corresponding to equilibrium points of (2.1)) are one-dimensional integral manifolds consisting of parallel straight lines as shown in Fig. 8(b).

2. The periodic solutions in Theorem 3.2 can be interpreted as one dimensional integral manifolds in the neighborhoods of straight-line manifolds of (2.1). See Fig. 8(b).

3. It follows from Theorems 3.1, 3.2 and Fig. 2(c) that for $\alpha_0(\beta) < \alpha < 1$ (3.1) has a two dimensional integral manifold S_ε as depicted in Fig. 8(a) as well as stable and unstable 1-dimensional integral manifolds as depicted in Fig. 8(b).

3.3 Integral manifold S_β associated with small β.

The following theorem shows that for sufficiently small β, the behavior of (3.1) is similar to that of the "reduced system"

$$\begin{aligned} \dot{x} &= y \\ 0 &= \alpha - \sin x - y - \varepsilon \sin \omega\tau \end{aligned} \tag{3.15}$$

obtained by setting $\beta = 0$ in (3.1).

Theorem 3.3 [3,9]

For β sufficiently small (3.1) has a stable integral manifold

$$S_\beta = \{(\tau,x,y) : y = \alpha - \sin x + \varepsilon \sin \omega\tau + f(\tau,x,\varepsilon,\beta),\ x \in \mathbb{R},\ \tau \in \mathbb{R}\} \tag{3.16}$$

where the function $f(\cdot,\cdot,\cdot,\cdot)$ satisfies the following properties:

(a) $f(\tau,x,\varepsilon,\beta)$ is smooth and bounded by D_β where $\lim_{\beta\to 0} D_\beta = 0$.

(b) $f(\tau,x,\varepsilon,\beta)$ is Lipschitzian in x with Lipschitz constant Δ_β, where $\lim_{\beta\to 0} \Delta_\beta = 0$.

(c) $f(\tau,x,\varepsilon,\beta)$ is 2π-periodic in x and $\frac{2\pi}{\omega}$ -periodic in τ.

Moreover for any initial condition on S_β, the solution of (3.1) can be obtained from the following equivalent system:

$$\dot{x} = \alpha - \sin x + \varepsilon \sin \omega\tau + f(\tau,x,\varepsilon,\beta) \tag{3.17a}$$

$$y = f(\tau,x,\varepsilon,\beta) + \alpha - \sin x + \varepsilon \sin \omega\tau \tag{3.17b}$$

Remarks:

1. The proof of this theorem is very similar to that of Theorem 3.1 and is outlined in Appendix D.

2. If both ε and β are small so that Theorems 3.1, 3.2, 3.3 hold simultaneously and $\beta < \beta_0(1)$ (so that $\alpha_0(\beta) = 1$) then:

a) for $\alpha > \alpha_0(\beta)$ both integral manifolds S_ε and S_β coincide. In this case $y = \psi(x)$ is close to $y = \alpha - \sin x$.

b) for $\alpha < \alpha_0(\beta)$ $\psi(x)$ ceases to exist and Theorem 3.1 does not apply.

In this case the stable and unstable periodic solutions alluded to in Theorem 3.2 must lie on the manifold S_β as shown in Fig. 9.

4. AC Analysis: Solutions on the Integral Manifold

4.1 Equation on torus

In this section we will discuss trajectories on manifolds S_ε and S_β. Due to Theorems 3.1 and 3.3, manifolds exist and are (asymptotically) stable. Hence, asymptotically-stable solutions on the manifold determine the steady state behavior of our system.

Now solutions on S_ε and S_β are determined by solving the scalar differential equations (3.7) and (3.17a), respectively. Once the solution corresponding to a given initial condition is found, the corresponding trajectory on S_ε and S_β

is uniquely specified by (3.6) and (3.17b), respectively. Consequently, it suffices to study the qualitative behaviors of (3.7) and (3.17a), which we will henceforth denote by:

$$\dot{\phi} = \frac{d\phi}{d\tau} = f(\tau,\phi) \tag{4.1}$$

$$f(\tau+\frac{2\pi}{\omega},\phi) = f(\tau,\phi), \quad f(\tau,\phi+2\pi) = f(\tau,\phi) \tag{4.2}$$

where ϕ denotes θ in (3.7) and x in (3.17a), and $f(\tau,\phi)$ denotes the corresponding expression on the right-hand side of (3.7) and (3.17a).†

Since each point (τ_0,ϕ_0) uniquely specifies a point on S_ε and S_β via (3.6) and (3.17b) respectively, we can use (τ,ϕ) to set up a coordinate system on S_ε and S_β. In particular, the locus of all points having identical first (respectively; second) coordinate defines a constant τ (respectively constant ϕ) curve as depicted in Fig. 10(a). Hence each point on S_ε and S_β is uniquely identified as the intersection between a constant-ϕ curve and a constant-τ curve.

Now consider the "grid" formed by the constant-ϕ_0 curves $\phi = \phi_0 + m \cdot 2\pi$ and constant-τ_0 curves $\tau = \tau_0 + n \cdot 2\pi$, $m,n = 0,\pm1,\pm2,\ldots$ where ϕ_0, τ_0 is any initial point. Since $f(\tau,\phi)$ is 2π-periodic in ϕ and $\frac{2\pi}{\omega}$-periodic in τ we can identify the constant-ϕ_0 curves and represent S_ε and S_β as a cylinder as shown in Fig. 10(b). Likewise, we can identify the constant-τ_0 curves (circular cross-sections in Fig. 10(b)) and represent S_ε and S_β as a torus as shown in Fig. 10(c).

Consequently, the qualitative behavior of (4.1) can be analyzed by the same technique as in [1].

However, unlike in [1] where $f(\tau,\phi)$ is explicitly given our $f(\tau,\phi)$ here, though exist in view of Theorems 3.1 and 3.3 is not available except that it satisfies (4.2). Fortunately most of the results in [1] depends only on this property and can be easily generalized.

4.2 Rotation Number μ

Let $\phi(\tau;\phi_0)$ denote any solution of (4.1) with $\phi(0;\phi_0) = \phi_0$. We define:

---

†The following results can be easily generalized to the case when the forcing function $\sin \omega t$ is replaced by any $\frac{2\pi}{\omega}$-periodic function. However, the results are not valid for almost-periodic excitations.

$$\mu := \frac{1}{\omega} \lim_{\tau\to\infty} \frac{\phi(\tau;\phi_0)}{\tau} \tag{4.3}$$

as the associated <u>rotation number</u>.[†]

<u>Theorem 4.1</u>: For any doubly-periodic equation (4.1) the <u>rotation number</u> μ defined by (4.3) exists and is independent of ϕ_0. Moreover the rotation number of (3.6) or (3.17a) is, apart from normalization constant, equal to the average voltage across the Josephson junction.

<u>Proof</u>: The existence and uniqueness of μ can be proved as in [5] (see also [1,12] for a different approach). To prove the average voltage interpretation consider first (3.6) where $\phi := \theta$. Since both $\psi'(\theta(\tau))$ and $h(\tau,\theta(\tau),\varepsilon)$ are bounded, (3.6a) implies

$$\lim_{\tau\to\infty} \frac{x(\tau)}{\tau} = \lim_{\tau\to\infty} \frac{\phi(\tau)}{\tau} = \mu\omega \tag{4.4}$$

The same relation holds trivially for (3.17a) where $\phi := x$. Now since $\dot{x}(\tau)$ has been identified in <u>Section 1</u> as the voltage across the Josephson junction,[††] the <u>average voltage</u> is:

$$\lim_{\tau\to\infty} \frac{1}{\tau} \int_0^\tau \dot{x}(\tau)d\tau = \lim_{\tau\to\infty} \frac{x(\tau)}{\tau} = \mu \cdot \omega \tag{4.5}$$

¤

<u>Remarks</u>:

1. Existence of average (4.5) is not obvious at all because even a bounded function may <u>not</u> have an average. For example the function

$$\dot{x}(\tau) = \sin(\ell n\ \tau),\ \tau \in [1,+\infty) \tag{4.6}$$

shown in Fig. 11 has <u>no average</u>. Indeed, since

$$q(T) := \frac{1}{T} \int_1^T \sin(\ell n\ \tau)d\tau = \frac{1}{2}[\sin(\ell n\ T) - \cos(\ell n\ T)] + \frac{1}{2T} \tag{4.7}$$

we have for $T_n = e^{n\pi}$,

[†] This corresponds to the "turning point" in [1] where ω was assumed to be unity.

[††] More exactly $v(t) = \frac{d\phi(t)}{dt}$ so $v(\tau/\Omega) = \Omega \frac{d\phi(\tau/\Omega)}{d\tau} = \Omega \cdot (\frac{4\pi e}{h})^{-1}\dot{x} = RI_c\dot{x}$.

Hence the average voltage $\bar{V} = \lim_{t\to\infty} \frac{1}{t}\int_0^t v(t)dt = \lim_{t\to\infty} \frac{\Omega}{t}\int_0^{t/\Omega} v(\frac{\tau}{\Omega})d\tau$

$= RI_c \lim_{t\to\infty} \frac{1}{\tau}\int_0^\tau \dot{x}(\tau)d\tau.$

$$q(T_n) = \frac{1}{2}[\sin(n\pi) - \cos(n\pi)] + \frac{1}{2}e^{-n\pi} = -\frac{1}{2}(-1)^n = \frac{e^{-n\pi}}{2} \quad (4.8)$$

Now choosing n = 2k and n = 2k + 1 respectively, we find:

$$\lim_{k\to\infty} q(T_{2k}) = -\frac{1}{2} + \frac{1}{2}e^{-2k\pi} = -\frac{1}{2} \quad (4.9)$$

and

$$\lim_{k\to\infty} q(T_{2k+1}) = -\frac{1}{2}(-1) + \frac{1}{2}e^{-(2k+1)\pi} = \frac{1}{2} \quad (4.10)$$

It follows from (4.9) and (4.10) that the average of the bounded waveform in Fig. 11 does not exist.

2. It was shown in [1,12] that the normalized average voltage μ can also be defined by a Dedekind cut in the set of rational numbers.

3. If we interpret $\phi(t)$ as a trajectory on the toroidal manifold in Fig. 10(c), then it follows from (4.4) and (4.5) that μ can be interpreted as the average angular velocity in which the trajectory rotates along the ϕ-direction on the torus. The larger μ is the faster the trajectory winds around the torus (along the ϕ-direction). This is the reason why μ is called rotation number.

4.3 Poincaré Map γ

Consider a cross-section C at some fixed time τ_0 on the torus of Fig. 10(c). For any point ϕ_0 on C, define the function

$$\gamma(\phi_0) := \phi(\tau_0 + \frac{2\pi}{\omega}; \phi_0) \quad (4.11)$$

Note that $\gamma(\phi_0)$ is simply the point where the trajectory starting from (τ_0,ϕ_0) returns and intersects C. For example in Fig. 12, P_0 maps into P_1 and P_1 maps into P_2. This return map is called the Poincaré map.

Higher iterations of Poincaré map can also be similarly defined as follow:

$$\gamma^n(\phi_0) := \gamma[\gamma^{n-1}(\phi_0)] = \phi(\tau_0 + n \cdot \frac{2\pi}{\omega}; \phi_0) \quad (4.12)$$

Example 1. $\dot{\phi} = \frac{\omega}{2}$ can be considered as an equation on the torus, where $(\tau,\phi) \in [0, \frac{2\pi}{\omega}] \times [0,2\pi]$. Since the solution is given by $\phi(\tau) = \frac{\omega}{2} + \phi_0 (\text{mod } 2\pi)$ (for $\tau_0 = 0$), the first and second iterations of the Poincaré map are given respectively by Figs. 13(a) and (b); namely

$$\gamma(\phi_0) = \phi(0 + \frac{2\pi}{\omega}; \phi_0) = \phi_0 + \pi \quad (\text{mod } 2\pi) \quad (4.13)$$

$$\gamma^2(\phi_0) = \phi(0 + \frac{4\pi}{\omega}; \phi_0) = \phi_0 + 2\pi = \phi_0 \quad (\text{mod } 2\pi) \tag{4.14}$$

Example 2. $\dot{\phi} = \sin\phi$ can be considered as an equation on the torus, where $(\tau,\phi) \in [0,\frac{2\pi}{\omega}] \times [0,2\pi]$. The solutions for this equation are shown in Fig. 14(a). Note that there are two constant solutions $\phi_1^* = 0$ and $\phi_2^* = \pi$. The Poincaré map constructed from these solution is shown Fig. 15(b). Note that $\gamma(\phi_0) > \phi_0$ for $\phi_0 \in (0,\pi)$ because the corresponding solutions in Fig. 15(a) are strictly increasing. On the other hand, $\gamma(\phi_0) < \phi_0$ for $\phi_0 \in (\pi,2\pi)$ because the corresponding solutions are strictly decreasing. Hence, ϕ_1^* is an unstable fixed point whereas ϕ_2^* is a stable fixed point of $\gamma(\phi_0)$.

Remarks:

1. Poincaré map γ is continuous and strictly increasing (because trajectories continuously depend on initital conditions and cannot intersect). Hence, γ preserves the orientation of the cross section C in Fig. 12.

2. A trajectory $\phi(\tau,\phi_0)$ of (4.1) is closed on the torus if and only if, there exist integers m and n such that $\phi(n\,\frac{2\pi}{\omega}, \phi_0) = \phi_0 + m2\pi$, i.e., $\gamma^n(\phi_0) = \phi_0$ (mod 2π).

3. The above remarks asserts that a trajectory $\phi(\tau,\phi_0)$ of (4.1) is periodic on the torus, if and only if, there exists some integer n such that the n-th iteration of Poincaré map has a fixed point.

4. It can also be shown that

$$\mu = \frac{1}{\omega} \lim_{n\to\infty} \frac{\gamma^n(\phi_0)}{n} \tag{4.15}$$

5. The following statements are easily shown to be equivalent:
   a. The rotation number of (4.1) is rational.
   b. There exist integer n such that γ^n has a fixed point.
   c. There exists a periodic trajectory on the torus.

6. If $\gamma^n(\phi_0)$ has at least one fixed point, and if $\frac{d}{d\phi_0}\gamma^n(\phi_0) \neq 1$ at all fixed points of $\gamma^n(\gamma_0)$, then all periodic solutions of (4.1) are isolated. Moreover stable and unstable periodic solutions of (4.1) must alternate.

7. If $\mu = \frac{p}{q}$, then the associated periodic trajectory must rotate around the torus (i.e., in the ϕ direction) p times before closing upon itself as τ increases from τ_0 to $\tau_0 + q\,\frac{2\pi}{\omega}$. In other words, $\phi(\tau + q\,\frac{2\pi}{\omega}) = \phi(\tau) + p2\pi$. A trajectory corresponding to p = 3 and q = 1 is shown on the surface S_ε or S_β in Fig. 15(a) and on the associated torus in Fig. 15(b). Note that the trajectory winds around the torus 3 times before closes upon itself.

4.4 Structural Stability

Consider (4.1) and a "perturbed" system

$$\dot{\phi} = f(\tau,\phi) + f_p(\tau,\phi) \tag{4.16}$$

where both $f(\cdot,\cdot)$ and $f_p(\cdot,\cdot)$ are smooth, 2π periodic in ϕ and $\frac{2\pi}{\omega}$ -periodic in τ. Let μ and μ_p denote the rotation number of (4.1) and (4.16), respectively.

Definition [12]: The rotation number μ of (4.1) is said to be stable iff it remains constant for all sufficiently small perturbations $f_p(\tau,\phi)$ i.e., $\mu = \mu_p$ for any $f_p(\cdot,\cdot)$ satisfying $\sup_{\tau,\phi}|f_p(\tau,\phi)| < \varepsilon$ where ε is "small enough".

Example 3: Consider Example 2 again. Since all solutions $\phi \neq 0$ of $\dot{\phi} = \sin\phi$ tend to $\phi + \pi$, its rotation number is:

$$\mu = \lim_{\tau\to\infty} \frac{\phi(\tau)}{\tau} = \lim_{\tau\to\infty} \frac{\pi}{\tau} = 0.$$

Consider next the perturbed equation

$$\dot{\phi} = \sin\phi + \varepsilon f_p(\tau,\phi) \tag{4.17}$$

where $\sup_{\tau,\phi}|f_p(\tau,\phi)| = 1$ and $f_p(\tau,\phi)$ is 2π-periodic in ϕ and $\frac{2\pi}{\omega}$ -periodic in τ. Consider the horizontal strip in the (τ,ϕ)-plane bounded by $|\phi| \leq \frac{3}{2}\pi$. Note that for sufficiently small ε (say $\varepsilon < \frac{1}{2}$) we have $\dot{\phi} = -1 + \varepsilon f_p(\tau,\frac{3}{2}\pi) < -\frac{1}{2}$ along the upper boundary $\phi = \frac{3\pi}{2}$. Conversely $\dot{\phi} = 1 + \varepsilon f_p(\tau,-\frac{3\pi}{2}) > \frac{1}{2}$ along the lower boundary $\phi = -\frac{3\pi}{2}$. Hence, all trajectories of (4.17) originating from points $\tau = 0$, $-\frac{3\pi}{2} < \phi < \frac{3\pi}{2}$ can never leave the strip. Consequently, the rotation number of (4.17) must satisfy $|\mu_p| = |\lim_{\tau\to\infty} \frac{\phi(\tau)}{\tau}| < \lim_{\tau\to\infty} \frac{3\pi}{2\tau} = 0$. Hence we have $\mu_p = 0 = \mu$ and the rotation number for $\dot{\phi} = \sin\phi$ is stable.

Whether the rotation number of (4.1) is stable or not is specified by the following result:

Theorem 4.2 [12]

Equation (4.1) has a stable rotation number if and only if, there exist a pair of integers p and q such that $\mu = p/q$ and the function $h(\phi_0) := \gamma^q(\phi_0) - \phi_0$ changes its sign at the fixed point of $\gamma^q(\phi_0)$.

Remarks:

1. Since $\mu = p/q$ corresponds to a periodic solution with period $q\frac{2\pi}{\omega}$, it follows that the q-th iterated Poincaré map $\gamma^q(\phi_0)$ has a fixed point ϕ_0^*.

2. A <u>rational</u> rotation number is <u>not necessarily</u> stable since $h(\phi_0)$ may not change sign at the fixed point ϕ_0^* of $\gamma^q(\phi_0)$ (e.g. $\dot{\phi} = \frac{\omega}{2}$ has rotation number $\frac{1}{2}$ which is obviously unstable and $h(\phi_0) := \gamma^2(\phi_0) - \phi_0 = 0$ for all ϕ_0).

4.5 Steady State Behavior

If we measure the average "dc" voltage V_{dc} as a function of the dc input current I_{dc} for the <u>nonautonomous</u> circuit, the resulting V_{dc} - I_{dc} characteristic was found to be step-wise constant and discontinuous as shown in Fig. 17, moreover each step is equal to a constant times a rational number. This strange characteristic, which differs drastically from that of Fig. 5 for the autonomous case, can now be rigorously explained with the help of following result:

<u>Theorem 4.3</u> AC Steady State Characterization.

Assuming (3.1) can be reduced to the study of an associated scalar differential equation (4.1) (i.e. either Theorem 3.1 or 3.3 holds) having a rotation number μ, then:

(a) If $\mu = m/n$, then the steady state solution of (3.1) satisfies the following periodicity relationship:

$$x(\tau + n\frac{2\pi}{\omega}) = x(\tau) + m2\pi \tag{4.18}$$

$$y(\tau + n\frac{2\pi}{\omega}) = y(\tau) \tag{4.19}$$

Consequently, the Josephson junction voltage is periodic with period $n\frac{2\pi}{\omega}$.

(b) If μ is irrational (and $f(\tau,\phi)$ is C^2) then any solution of (3.1) on S_ε or S_β can be written in the form:

$$x(\tau) = \mu\omega\tau + g_1(\omega\tau,\mu\omega\tau) \tag{4.20}$$

$$y(\tau) = g_2(\omega\tau,\mu\omega\tau) \tag{4.21}$$

where both functions $g_1(\omega\tau,\mu\omega\tau)$ and $g_2(\omega\tau,\mu\omega\tau)$ are 2π-periodic in $\omega\tau$ <u>and</u> $\mu\omega\tau$.†

<u>Proof</u>:

(a) If μ is rational, then it follows from Remark 5 of Section 4.3 that 4.1 has a periodic solution (mod 2π) satisfying $\phi(\tau + n\frac{2\pi}{\omega}) = \phi(\tau) + m2\pi$.

If (3.1) has an integral manifold S_ε (small-ε case) then $\phi = \theta$ and (3.6) holds. Since $\psi(\theta)$, $\psi'(\theta)$ and $h(\tau,\theta(\tau),\varepsilon)$ are 2π-periodic in θ and $\frac{2\pi}{\omega}$-periodic

---

†Statement (a) can be considered as a special case of statement (b). Indeed if μ is <u>rational</u>, then the two frequencies ω and $\mu\omega$ are commensurable and hence both $\overline{x(\tau) - \mu\omega\tau}$ and $y(\tau)$ are periodic.

in τ, it follows that $x(\tau)$ and $y(\tau)$ must satisfy (4.18)-(4.19). Similarly, if (3.1) has an integral manifold S_β (small-β case) then $\phi = x$ and (3.17b) holds. Again, since $f(\tau,x,\varepsilon,\beta)$ is 2π-periodic in θ and $\frac{2\pi}{\omega}$ -periodic in τ, (4.18)-(4.19) must hold.

(b) Since $f(\tau,\phi)$ is twice continuously differentiable it follows from Bohl's theorem in [5, page 414] that there exists a continuous function $g(\tau,\phi)$ such that any solution of (4.1) can be written in the form:

$$\phi(\tau) = \mu\omega\tau + \phi_0 + g(\tau,\mu\omega\tau + \phi_0) \tag{4.22}$$

where $g(\tau,\phi)$ is 2π-periodic in ϕ and $\frac{2\pi}{\omega}$ -periodic in τ, and ϕ_0 is a constant. Applying once again (4.22) into (3.6) or (3.17b) we obtain (4.20)-(4.21). ¤

4.6 Explanation of the Voltage-Step Phenomena

Since the rotation number μ of (4.1) is equal to the normalized average Josephson junction voltage (Theorem 4.1), it follows from Theorem 4.2 that if the average voltage remains constant (as a function of I_{dc}) for small changes in I_{dc} then it must be equal to $\omega \cdot \frac{p}{q}$ (ω times some rational number). This result is consistent† with experiment (Fig. 17). Note that only those rotation numbers p/q which also satisfy the second condition in Theorem 4.2 will give rise to constant voltage steps.

For example, the periodic solutions of the autonomous system (2.1) do not give rise to any horizontal voltage steps (Fig. 5). Indeed we can state the following two corollaries:

Corollary 4.1:

The rotation number associated with the invariant manifold S_0 of the autonomous system (2.1) is always unstable and hence no non-zero voltage can appear in Fig. 5.

Proof: Substituting $\varepsilon = 0$ in (3.4a) we obtain

$$\dot{\theta} = \psi(\theta) \tag{4.23}$$

where $\psi(\theta)$ is 2π-periodic in θ and strictly positive for all θ, and can be considered as $\frac{2\pi}{\omega}$ -periodic in τ, for any ω. Now any solution of (4.23) is of the form

†Rotation number (and an average voltage) is a continuous function of I_{dc}. However, the waveforms corresponding to unstable μ or "short steps" of μ cannot be observed experimentally. Hence, the experimental characteristics in Fig. 17 is discontinuous.

$$\theta(\tau) = \frac{2\pi}{T}\tau + p(\tau) \tag{4.24}$$

where $T := \int_0^{2\pi} \frac{dx}{\psi(x)}$ and $p(\tau)$ is T-periodic. (Property 3 of Section 2.2). Hence, the rotation number of (4.23) is

$$\mu = \frac{1}{\omega} \lim_{\tau\to\infty} \frac{\theta(\tau)}{\tau} = \frac{2\pi}{\omega T} = \frac{2\pi}{\omega}\left(\int_0^{2\pi} \frac{dx}{\psi(x)}\right)^{-1} \tag{4.25}$$

Similarly, the rotation number μ_p of the perturbed equation

$$\dot{\theta} = \psi(\theta) + \eta \tag{4.26}$$

is given by

$$\mu_p = \frac{2\pi}{\omega}\left(\int_0^{2\pi} \frac{dx}{\psi(x)+\eta}\right)^{-1} \tag{4.27}$$

provided $\psi(x) + \eta > 0$. It follows from (4.25) and (4.27) that $\mu_p \neq \mu$ and hence μ of (4.23) is unstable. ¤

Corollary 4.2

The rotation number associated with the invariant manifold S_β of the autonomous system (2.1) with sufficiently small β is either unstable or zero.

Proof: Substituting $\varepsilon = 0$ in (3.17a) for the small-β case we obtain

$$\dot{x} = \alpha - \sin x + \hat{f}(x,\beta) \tag{4.28}$$

where $\hat{f}(x,\beta) := f(0,x,0,\beta)$† is 2π-periodic in x and bounded by D_β where $D_\beta \to 0$ with $\beta \to 0$.

Now as long as $\alpha > 1 + D_\beta$ so that (4.28) has no equilibrium point, (4.28) can be analyzed by the same method as (4.23); namely it has a solution of the form

$$x(\tau) = \frac{2\pi}{T_1}\tau + p_1(\tau) \tag{4.29}$$

where $T_1 := \int_0^{2\pi} \frac{dx}{\alpha - \sin x + \hat{f}(x,\beta)}$ and $p_1(\tau)$ is T_1-periodic. Hence, the rotation number of (4.33) is unstable.

---

†For $\varepsilon = 0$ $f(\tau,x,\varepsilon,\beta)$ does not depend on τ so $f(\tau,x,0,\beta) = f(0,x,0,\beta)$.

On the other hand if $\alpha < 1 - D_\beta$ and (4.28) has an equilibrium point x_0, i.e., $\alpha - \sin x_0 + f(x_0,\beta) = 0$ then $\mu = \frac{1}{\omega} \lim_{\tau\to\infty} \frac{x(\tau)}{\tau} = \frac{1}{\omega} \lim \frac{x_0}{\tau} = 0$.

Note that for $\alpha < 1$ and β small enough (4.28) has always equilibrium point x_0 (since $D_\beta \to 0$ as $\beta \to 0$). Hence, μ is equal to zero and does not change under small changes of α (as long as $\alpha < 1$ and β remains small). This confirms zero voltage-step characteristic in Fig. 5. For $|I_{dc}| > I_0$ + "small" term (what corresponds to $\alpha > 1 + D_\beta$), the rotation number is no longer stable and no voltage step appears in this region.†

†Since β must be small in this analysis, Corollary 4.2 does not predict the hysteresis phenomenon in Fig. 5.

REFERENCES

[1] A. A. Abidi, and L. O. Chua, "On the dynamics of Josephson-junction circuits," Electronic Circuits and Systems, Vol. 3, pp. 186-200, July 1979.

[2] A. A. Andronov, S. E. Khaikin, and A. A. Vitt, Theory of Oscillators, Pergamon Press, New York, 1966.

[3] Ya. S. Baris, V. I. Fodchuk, "Bounded solutions in nonlinear singularity perturbed systems via integral manifolds," Ukr. Math. Journal, Vol. 22, No. 1, pp. 3-11, 1970 (in Russian).

[4] N. N. Bogoliubov and Y. A. Mitropolskii, Asymptotic Methods in the Theory of Nonlinear Oscillations, Gordon and Breach, New York, 1961.

[5] E. A. Coddington and N. Levinson, Theory of Ordinary Differential Equations, McGraw-Hill, New York, 1955.

[6] C. M. Falco, "Phase-space of a driven, damped pendulum (Josephson weak link)," Am. Journal of Physics, 44, pp. 733-74, 1976.

[7] J. K. Hale, Ordinary Differential Equations, R. Krieger, New York, 1980.

[8] M. Levi, F. C. Hoppensteadt, and W. L. Miranker, "Dynamics of the Josephson junction," Quarterly of Appl. Math., pp. 167-198, July 1978.

[9] Y. A. Mitropolskii and O. B. Lykova, Integral Manifolds in Nonlinear Mechanics, Nauka, Moscow, 1973 (in Russian).

[10] D. E. McCumber, "Effect of a.c. impedance on d.c. voltage-current characteristics of superconductor weak-link junctions," J. Appl. Phys., Vol. 39, pp. 3113-3118, 1968.

[11] B. Montandon,"Almost periodic solutions and integral manifolds for weakly nonlinear nonconservative systems," J. Differential Equations, Vol. 12, 417-425, 1972.

[12] V. A. Pliss, Nonlocal Problems of the Theory of Oscillations, Academic Press, New York, 1966.

[13] S.Q.U.I.D., Proceedings of the International Conference on Superconducting Quantum Devices, Berlin, 1976 (1st Conference), 1980 (2nd).

[14] J. R. Waldram, "A. B. Pippard, and J. Clarke, "Theory of the current-voltage characteristics of SNS junctions and other superconducting weak links," Philos. Trans. Roy. Soc. London, Vol. 268A, pp. 265-287, 1970.

APPENDIX

A. Outline of phase-plane analysis

We shall briefly discuss the Andronov-Vitt-Khaikin [2] proof of the existence of a periodic (in x) trajectory $y = \psi(x)$.

Note that trajectories of (2.1) in the (x,y)-plane coincide[†] with solutions of

$$\frac{dy}{dx} = -a + \frac{b - \sin x}{y} \tag{A.1}$$

The right hand side of (A.1) is 2π-periodic in x so instead of x-y plane it is enough to consider only a vertical strip of width 2π $\{(x,y) : x_0 < x < x_0 + 2\pi$ $y \in \mathbb{R}\}$ where x_0 may be arbitrarily chosen (Fig. A1). Let $y(x) := y(x;x_0,y_0)$ denote the solution of (A.1) with initial condition $y(x_0) = y_0$. Note that for y_0 large enough $y(x_0+2\pi;x_0,y_0) < y_0$ (since $\frac{dy}{dx} < 0$ for large y).

If we show that for "small" positive y_0[††], $y(x_0+2\pi;x_0,y_0) > y_0$, then continuous dependence of trajectories on initial conditions yields existence of $\bar{y}_0$ such that $y(x_0+2\pi;x_0,\bar{y}_0) = \bar{y}_0$. So there exists $\psi(x) := y(x;x_0,\bar{y}_0)$ which is 2π-periodic in x and stable.

It can be shown [2] moreover, that $\psi(x)$ is a unique periodic trajectory of (2.1) (as a consequence of Bendixon's criterion).

In the case $b > 1$ it is easy to find small $y_0 \geq 0$ for which $y(x_0+2\pi) > y_0$ (it is enough to take $0 < y_0 < \min_x(b - \sin x) = b - 1$). In the case $b \leq 1$ we choose $x_0 = \pi - \sin^{-1} b$, i.e., the left boundary of the vertical strip passes through the saddle point (or saddle-node for $b = 1$). Consider the separatrix originating from the saddle and going upwards.

Let a be fixed, then for $b = 0$ the separatrix tends to the stable equilibrium point (Fig. A.2a) and does not reach the line $x = x_0 + 2\pi$. On the other hand, for $b = 1$ (Fig. A.2d), the separatrix does cross the vertical line $x = x_0 + 2\pi$ at a positive value of y.

[†]More exactly, for $b := \alpha$, $a = \beta^{-1/2}$, $\tau = a^{-1}t$, (A.1) is equivalent to (2.1) for $y \neq 0$; for $y = 0$, i.e., on x-axis trajectories of (2.1) are vertical.

[††]For $b > 0$ and $a > 0$ the periodic trajectory of (A.1) may exist only in the upper half-plane [2].

Since trajectories depend continuously on parameters the phase portrait for small b is similar to that when b = 0 (Fig. A.2a). For $b < 1$, but close to 1, we get the portrait shown in Fig. A.2c. Moreover, there exist $b_0 \in (0,1)$ such that for $b = b_0$ the separatrix joins two saddles (Fig. A.2b).

Obviously b_0 is uniquely defined (for $\frac{dy}{dx}$ increases with b for any fixed $a > 0$, $y > 0$, x) and does continuously depend on a (for the trajectories depend continuously on parameters).

To stress the dependence of b_0 on a we shall write $b_0 = b_0(a)$. So for any $a > 0$ and $b > b_0(a)$ the system (A.1) (and also (2.1)) passes in x-y plane the unique 2π-periodic trajectory $y = \psi(x)$.

Proof of Property 2

Consider (A.1) with $b = b_1$

$$\frac{dy}{dx} = -a + \frac{b_1 - \sin x}{y} \tag{A.2}$$

and with $b = b_2$

$$\frac{dy}{dx} = -a + \frac{b_2 - \sin x}{y} \tag{A.3}$$

let $b_2 > b_1 > b_0(a)$ and let $y_{ab_1}(x;x_0,y_0)$, $\psi_{ab_1}(x)$, and $y_{ab_2}(x;x_0,y_0)$, $\psi_{ab_2}(x)$ denote trajectories of (A.2) and (A.3) respectively. Since $b_1 > b_0(a)$ there exist $\psi_{ab_1}(x)$. Consider the trajectory $y_{ab_2}(x)$ of (A.3) starting from $x = x_0$, $y = \psi_{ab_1}(x_0)$ (Fig. A3). Since for any $x,y > 0$, $a > 0$, $\frac{dy}{dx}$ is larger for $b = b_2$ than for $b = b_1$ and since $y_{ab_2}(x_0+2\pi;x_0,\psi_{ab_1}(x_0)) > \psi_{ab_1}(x_0)$, it follows that $\psi_{ab_2}(x)$ must lie above $y_{ab_2}(x)$ and $\psi_{ab_2}(x) > \psi_{ab_1}(x)$ for any x. In a similar way we prove that for fixed b and $a_1 > a_2$, $\psi_{a_1b}(x) < \psi_{a_2b}(x)$ for any x if only ψ_{a_1b} and ψ_{a_2b} exist i.e., if $b > b_0(a_1)$.

Finally the transformation $\alpha := b$, $\beta = a^{-2}$ yields Property 2.

Proof of Property 1

We have already shown that $b_0 = b_0(a)$ is a continuous function of a $a \in (0,+\infty)$ The same reasoning shows that $b_0(a)$ is monotonically increasing. Indeed for given a_1 and $b = b_0(a_1)$ the separatrix passes as in the Fig. A.2(b). If we take $a_2 > a_1$ it will not reach the vertical line $x = x_0 + 2\pi$ in Fig. A.1(a). Hence, the crtical value of b for a_2 is larger then $b_0(a_1)$, i.e., $b_0(a_2) > b_0(a_1)$.

The behavior of trajectories yields also $\inf_{a>0} b_0(a) = 0$ (since for any $b' \in (0,1)$ we can find a' "small" such that for $a = a'$ and $b = b'$ the phase portrait is as in the Fig. A.2(c), i.e., $b_0(a') < b'$), $\sup_{a>0} b_0(a) = 1$ (for any $b'' \in (0,1)$ we can find a" "large" such that for $a = a''$, $b = b''$, the phase portrait is as in the Fig. A-2a, i.e., $b_0(a'') > b''$). Since $b_0(a)$ increases monotonically with a we get

$$\lim_{a\to 0} b_0(a) = \inf b_0(a) = 0, \quad \lim_{a\to\infty} b_0(a) = \sup b_0(a) = 1$$

Hence, Property 1 is proved.

Remark

Note that since the right hand sides of (A.1) and (2.1) are 2π-periodic, we can identify in the x-y plane the vertical lines $x = x_0 + 2k\pi$, $k = 0,\pm1,\pm2,\ldots$; and instead of the x-y plane, or the vertical strip, we can consider the cylinder in Fig. A4. The trajectory $y = \psi(x)$ which is periodic in x in the plane becomes periodic also in time when considered on the surface of the cylinder.

Warning. In Section 2 of this paper, we consider another cylindrical surface S_0 of solutions of (2.1) (Fig. 4(b)). This surface S_0 (although cylinder) involves a different concept from the one considered above.

B. New coordinates

Consider

$$\dot{x} = y$$
$$\beta y = \alpha - \sin x - y + \varepsilon q(t) \qquad (B.1)$$

and introduce new coordinates θ, ρ

$$x =: \theta - \psi'(\theta)\rho$$
$$y =: \psi(\theta) + \rho \qquad (B.2)$$

where $\psi(\theta)$ is 2π-periodic solution of

$$y'(\theta) = -\frac{1}{\beta} + \frac{\alpha - \sin\theta}{\beta y(\theta)} \qquad (B.3)$$

We shall show that in new variables the equations (B.1) take the form

$$\dot{\theta} = \psi(\theta) + \rho G(\theta,\rho) + \varepsilon P(t,\theta,\rho)$$
$$\dot{\rho} = A(\theta)\rho + \rho^2 F(\theta,\rho) + \varepsilon Q(t,\theta,\rho) \qquad (B.4)$$

To avoid writing long formulas, let us introduce:

$$Y(x,y) := \frac{1}{\beta}[\alpha - \sin x - y]$$
$$\bar{q}(t) := \frac{\varepsilon}{\beta} q(t) \qquad (B.5)$$

under this notation, (B.1) is reduced to:

$$\dot{x} = y$$
$$\dot{y} = Y(x,y) + \bar{q}(t) \qquad (B.6)$$

Substituting (B.2) into (B.6), we obtain:

$$[1-\rho\psi''(\theta)]\dot{\theta} - \psi'(\theta)\dot{\rho} = \psi(\theta) + \rho$$
$$\psi'(\theta) \cdot \dot{\theta} + 1 \cdot \rho = Y(\theta-\rho\psi'(\theta),\psi(\theta)+\rho) + \bar{q}(t) \qquad (B.7)$$

Equations (B.7) are linear with respect to $\dot{\theta}$ and $\dot{\rho}$ and its determinant is given by:

$$D(\theta,\rho) = 1 + [\psi'(\theta)]^2 - \rho\psi''(\theta).$$

Hence, for small ρ, $D(\theta,\rho) > 0$. Solving (B.7) we get:

$$\dot{\theta} = [\psi + \psi^1 \cdot Y(\theta - \rho\psi^1, \psi + \rho) + \psi^1 \cdot \bar{q}]/D(\theta,\rho)$$

$$\dot{\rho} = \{[1 - \rho\psi''] \cdot [Y(\theta - \rho\psi^1, \psi + \rho) + \bar{q}] - \psi^1 \cdot [\psi + \rho]\}/D(\theta,\rho) \qquad \text{(B.8)}$$

where in the formulas above, we write $\bar{q}$, ψ, ψ', ψ'' instead of $\bar{q}(t)$, $\psi(\theta)$, $\psi'(\theta)$, $\psi''(\theta)$. Let us develop Y with respect to ρ:

$$Y(\theta - \rho\psi', \psi + \rho) = Y - \rho[Y_{,1} \cdot \psi' + Y_{,2}] + \rho^2 Y_{,11}\,[Y']^2 + O(\rho^3) \qquad \text{(B.9)}$$

where

$$Y := Y(\theta,\psi) = \frac{1}{\beta}[\alpha - \sin\theta - \psi]$$

$$Y_{,1} = \frac{\partial}{\partial x} Y(x,y)\Big|_{\substack{x=\theta\\ y=\psi}} = -\frac{1}{\beta}\cos\theta$$

$$Y_{,11} = \frac{\partial^2}{\partial x^2} Y(x,y)\Big|_{\substack{x=\theta\\ y=\psi}} = \frac{1}{\beta}\sin\theta$$

$$Y_{,2} = \frac{\partial}{\partial y} Y(x,y)\Big|_{\substack{x=\theta\\ y=\psi}} = -\frac{1}{\beta}$$

$O(\rho^k)$ denote the function $f(\rho,\ldots)$ such that $\lim\limits_{\rho\to 0} \frac{f(\rho,\ldots)}{\rho^k}$ is bounded. Applying (B.9) to (B.8) we get:

$$\dot{\theta} = \{\psi + \psi' \cdot Y + \rho[1 - [\psi']^2 Y_{,1} + \psi' \cdot Y_{,2}] + O(\rho^2)\}/D(\theta,\rho) + \frac{\psi'}{D(\theta,\rho)} \cdot \bar{q} \qquad \text{(B.10)}$$

$$\dot{\rho} = \{Y - \psi \cdot \psi' - \rho[\psi' + \psi'' \cdot Y + \psi' Y_{,1} - Y_{,2}] + \rho^2[\psi'\psi'' Y_{,1} - \psi'' Y_{,2} + [\psi']^2 \cdot Y_{,11}]$$

$$+ O(\rho^3)/D(\theta,\rho) + \frac{1-\rho\psi''}{D(\theta,\rho)} \cdot \bar{q} \qquad \text{(B.11)}$$

Note that $\psi(\theta)$ is solution of (B.3) so:

$$\psi(\theta)\psi'(\theta) = Y(\theta,\psi(\theta))$$

$$\psi'(\theta) \cdot Y[\theta,\psi(\theta)] = \psi(\theta) \cdot [\psi'(\theta)]^2$$

and

$$D^{-1}(\theta,\rho) = \{1 + [\psi']^2 - \rho\psi''\}^{-1} = \frac{1}{1+[\psi']^2} + \frac{\rho\psi''}{(1+[\psi']^2)} + \frac{\rho^2(\psi'')^2}{(1+[\psi']^2)^3} + \ldots$$

So equation (B.10) can be reduced to

$$\dot{\theta} = \psi(\theta) + \rho G(\theta,\rho) + \varepsilon P(t,\theta,\rho) \qquad \text{(B.12)}$$

where

$$P(t,\theta,\rho) := \frac{1}{\beta} \cdot q(t) \cdot \frac{1 - \rho\psi''(\theta)}{1 + [\psi'(\theta)]^2 - \rho\psi''(\theta)}$$

$$G(\theta,\rho) := \frac{\psi''(\theta) + 1 - [\psi'(\theta)]^2 Y,_1(\theta,\psi) + \psi'(\theta)Y,_2(\theta,\psi)}{1 + [\psi'(\theta)]^2} + O(\rho)$$

$$= \frac{1 + \psi''(\theta) + \frac{1}{\beta}[\psi'(\theta)]^2 \cos\theta - \frac{1}{\beta} \cdot \psi'(\theta)}{1 + [\psi'(\theta)]^2}$$

Equation (B.11) can be reduced to:

$$\dot{\rho} = A(\theta)\rho + \rho^2 F(\theta,\rho) + \varepsilon Q(t,\theta,\rho) \qquad \text{(B.13)}$$

where

$$Q(t,\theta,\rho) := \frac{1}{\beta} \cdot q(t) \cdot \frac{1 - \rho\psi''(\theta)}{1 + [\psi'(\theta)]^2 - \rho\psi''(\theta)}$$

$$A(\theta) := -\frac{\psi' + \psi'' \cdot Y + \psi' Y,_1 - Y,_2}{1 + [\psi']^2}$$

$$= \frac{\psi'' Y + \psi' + \psi' Y,_1 + [\psi']^2 Y,_2 - Y,_2 \cdot (1 + [\psi']^2)}{1 + [\psi']^2}$$

$$= \psi'(\theta) + Y,_2(\theta,\psi) - 2\frac{\psi''(\theta) \cdot Y(\theta,\psi)}{1 + [\psi'(\theta)]^2}$$

$$= -\frac{1}{\beta} + \psi'(\theta) + \frac{1}{\beta}\frac{2\psi''(\theta)}{1 + [\psi'(\theta)]^2}[\alpha - \sin\theta - \psi(\theta)]$$

$$= -\frac{1}{\beta}\frac{\alpha - \sin\theta}{\psi(\theta)} + \frac{2\psi''(\theta)}{1 + [\psi'(\theta)]^2}[\alpha - \sin\theta - \psi(\theta)]$$

$$F(\theta,\rho) := \frac{\psi''}{(1 + [\psi']^2)^2} \cdot [\psi' + \psi'' \cdot Y + \psi' Y,_1 - Y,_2]$$

$$+ \frac{1}{1 + [\theta']^2}[\psi'\psi'' Y,_1 - \psi'' Y,_2 + [\psi']^2 Y,_{11}] + O(\rho) = \frac{\psi''(\theta)}{1 + [\psi'(\theta)]^2} \cdot A(\theta)$$

$$+ \frac{1}{1 + [\psi'(\theta)]^2}[-\psi'(\theta)\psi''(\theta)\frac{\cos\theta}{\beta} + \frac{1}{\beta}\psi''(\theta) + \frac{1}{\beta}[\psi'(\theta)]^2\psi''(\theta)$$

$$+ O(\rho)$$

Note that

$$\psi'(\theta) = \frac{Y(\theta,\psi)}{\psi} = \frac{1}{\beta\psi(\theta)}[\alpha - \sin\theta - \psi(\theta)]$$

and

$$\psi''(\theta) = \frac{(Y_{,1} + Y_{,2} \cdot \psi')\psi - \psi' \cdot Y}{\psi^2}$$

$$= \frac{1}{\psi} Y_{,1} + \frac{1}{\psi^2} Y \cdot Y_{,2} - \frac{1}{\psi^3} Y$$

$$= - \frac{1}{\beta\psi(\theta)} \cos\theta + \frac{\alpha - \sin\theta - \psi(\theta)}{\beta[\psi(\theta)]^2} \cdot [\alpha - \sin\theta]$$

Hence, for small ρ, the equations (B.6) are equivalent to

$$\begin{aligned} \dot{\theta} &= \psi(\theta) + \bar{G}(t,\theta,\rho,\varepsilon) \\ \dot{\rho} &= A(\theta)\rho + \bar{F}(t,\theta,\rho,\varepsilon) \end{aligned} \qquad \text{(B.14)}$$

where

$$\bar{G}(t,\theta,\rho) := \rho G(\theta,\rho) + \varepsilon P(t,\theta,\rho)$$

$$F(t,\theta,\rho) := \rho^2 F(\theta,\rho) + \varepsilon Q(t,\theta,\rho)$$

are small for small ρ and small ε.

C. Remarks and references for proof of Theorem 3.1

Consider equations

$$\dot{\theta} = \psi(\theta) + G(\tau,\theta,\rho,\varepsilon)$$
$$\dot{\rho} + A(\theta)\rho + F(\tau,\theta,\rho,\varepsilon) \qquad \text{(C.1)}$$

Step 1 We will outline the proof in 4 steps:

Introduce new variable $\bar{\theta} := \int_0^\theta \frac{d\theta}{\psi(\theta)}$

Note that $\frac{d\bar{\theta}}{d\theta} = \frac{1}{\psi(\theta)}$ and since $\psi(\theta) > 0$ for any θ, $\bar{\theta}(\theta)$ is 1:1 function. Let $\theta(\theta)$ denote its' inverse. Hence, equations (C.1) are equivalent to

$$\theta = 1 + \bar{G}(\tau,\bar{\theta},\rho,\varepsilon) \qquad \text{(C.2a)}$$

$$\dot{\rho} = \bar{A}(\bar{\theta})\rho + \bar{F}(\tau,\bar{\theta},\rho,\varepsilon) \qquad \text{(C.2b)}$$

with

$$\bar{G}(\tau,\bar{\theta},\rho,\varepsilon) := \frac{1}{\psi(\theta(\bar{\theta}))} G(\tau,\theta(\bar{\theta}),\rho,\varepsilon)$$

$$\bar{A}(\bar{\theta}) := A(\theta(\bar{\theta})), \; \bar{F}(\tau,\bar{\theta},\rho,\varepsilon) = F(\tau,\theta(\bar{\theta}),\rho,\varepsilon)$$

It follows immediately from Appendix B that for $\rho \in [0,v)$ and v small enough the functions $A(\theta)$, $\bar{G}(\tau,\bar{\theta},\rho,\varepsilon)$, $\bar{F}(\tau,\bar{\theta},\rho,\varepsilon)$ are:

1) bounded and smooth in all the variables

2) $\bar{A}$, $\bar{G}$, $\bar{F}$ are Lipschitzian in θ with Lipschitz constants λ, $\gamma(v,\varepsilon)$, and $\eta(v,\varepsilon)$ respectively where $\gamma(v,\varepsilon)$ $\eta(v,\varepsilon)$ are nondecreasing functions of v,ε and $\eta(v,\varepsilon) \to 0$

3) $\bar{G}$, $\bar{F}$ are Lipschitzian in ρ with Lipschitz constants $M + \mu(v,\varepsilon)$ and $\mu(v,\varepsilon)$ respectively and $\mu(v,\varepsilon) \to 0$ as $v,\varepsilon \to 0$.

4) $\bar{G}(\tau,\bar{\theta},0,\varepsilon)$, $\bar{F}(\tau,\bar{\theta},0,\varepsilon)$ are bounded with $N(\varepsilon)$ where $N(\varepsilon) \underset{\varepsilon\to 0}{\longrightarrow} 0$

Step 2

Consider the "unperturbed" system (C.2)

$$\dot{\bar{\theta}} = 1 \qquad \text{(C.3a)}$$

$$\dot{\rho} = \bar{A}(\bar{\theta})\rho \qquad \text{(C.3b)}$$

Solution of (C.3(a)) is given explicitly by $\bar{\theta}(\tau) = \tau + \phi$, where ϕ is a constant. Hence, solution of (C.3b) is of the form

$$\rho(\tau) = \rho(\tau;\tau_0,\rho_0) = e^{\int_{\tau_0}^{\tau} \bar{A}(s+\phi)ds} \rho_0$$

Since $\bar{A}(s) = A(\theta(s))$ is T-periodic in s we get:

$$\int_{\tau_0}^{\tau} \bar{A}(s+\phi)ds = (\tau-\tau_0)A_0 + Q(\tau)$$

where

$$A_0 := \int_0^T \bar{A}(s)ds$$

$$Q(\tau) := \int_{\tau_0}^{\tau} \bar{A}(s+\phi)ds - (\tau-\tau_0)A_0 \text{ is T-periodic in } \tau$$

Note that

$$A_0 = \frac{1}{T}\int_0^T A(s)ds = \frac{1}{T}\int_0^T A(\theta(s))ds = \begin{matrix}\text{by definition of}\\ A(\theta) \text{ in Appendix B}\end{matrix} =$$

$$= \frac{1}{T}\int_0^T -\frac{1}{\beta} + \psi'(\theta(s)) + \frac{2\psi'(\theta(s))\psi''(\theta(s))\psi(\theta(s))}{1+[\psi'(\theta(s))]^2} ds =$$

$$= \left|\frac{d\theta}{ds} = \psi(\theta(s))\right| = -\frac{1}{\beta} - \frac{1}{T}\int_0^{2\pi} \frac{\psi'(\theta)}{\psi(\theta)} d\theta - \frac{1}{T}\int_0^{2\pi} \frac{\psi''(\theta)\psi'(\theta)d\theta}{1+[\psi'(\theta(s))]^2}$$

$$= -\frac{1}{\beta} - (\frac{1}{T}\log x)\Big|_{\psi(0)}^{\psi(2\pi)} - \frac{1}{T}(\log 1 + x)\Big|_{[\psi'(0)]^2}^{[\psi'(2\pi)]^2}$$

Define $K := \sup_{\tau}|e^{Q(\tau)}|$, under this notation

$$|\rho(\tau,\tau_0,\rho_0)| = |e^{A_0(\tau-\tau_0)}e^{Q(\tau)}\rho_0| \leq K e^{-\frac{\tau-\tau_0}{\beta}} |\rho_0| \quad \text{(C.4)}$$

<u>Step 3</u>

It can be proved [11] that if conditions 1-4 (step 1) and inequality (C.4) are satisfied, then equations (C.2) possesses a smooth integral manifold $\bar{S}_\varepsilon = \{(\tau,\bar{\theta},\rho) : \rho = \bar{h}(\tau,\bar{\theta},\varepsilon)\}$ and for appropriately chosen initial conditions they are equivalent to:

$$\dot{\bar{\theta}} = 1 + G(\tau,\bar{\theta},\bar{h}(\tau,\bar{\theta},\varepsilon))$$

$$\rho(t) = h(\tau,\bar{\theta},\varepsilon)$$

Step 4

Since the transformation $\theta \leftrightarrow \bar{\theta}$ is one-to-one and smooth (for $\psi(\theta)$ is a smooth function) (C.1) possesses an integral manifold

$$S_\varepsilon = \{(\tau,\theta,\rho) : \rho = h(\tau,\theta,\varepsilon),\ \tau \in \mathbb{R},\ \theta \in \mathbb{R}\}$$

where

$$h(\tau,\theta,\varepsilon) := \bar{h}(\tau,\bar{\theta}(\theta),\varepsilon).$$

Hence, for any initial condition on the manifold, (C.1) is equivalent to:

$$\dot{\theta} = \psi(\theta) + G(\tau,\theta,h(\tau,\theta,\varepsilon),\varepsilon).$$

D. Outline of the proof of Theorem 3.3

Introducing new coordinates

$$x := x$$
$$z := u - \alpha + \sin x - \varepsilon \sin \omega\tau \qquad (D.1)$$

in (3.1a,b) we obtain:

$$\dot{x} = y = z + \alpha - \sin x + \varepsilon \sin \omega\tau$$

$$\beta\dot{z} = \beta(\dot{y} - \cos x \cdot \dot{x}\, \varepsilon\omega \cos \omega\tau) = \alpha - \sin x - y + \varepsilon \sin \omega\tau$$
$$- \beta \cos x \cdot y - \varepsilon\beta\omega \cos \omega\tau$$

Hence

$$\dot{x} = z + \alpha - \sin x + \varepsilon \sin \omega\tau \qquad (D.2a)$$

$$\dot{z} = -\frac{1}{\beta} z - \{\cos x[z + \alpha - \sin x + \varepsilon \sin \omega\tau] + \varepsilon\omega \cos \omega\tau\} \qquad (D.2b)$$

Similarly as before we introduce function space $C(D_\beta,\Delta_\beta)$ as "candidates for manifold". The elements $F(t,x,\beta,\varepsilon)$ of $C(D_\beta,\Delta_\beta)$ are smooth, bounded with D_β, $\frac{2\pi}{\omega}$-periodic in τ, 2π periodic and Δ_β-Lipschitzian in x where $D_\beta \to 0$, $\Delta_\beta \to 0$ as $\beta \to 0$.

Let $x^F(\tau) = x^F(\tau;\tau_0,x_0)$ denote solution of

$$\dot{x} = F(\tau,x,\beta,\varepsilon) + \alpha - \sin x + \varepsilon \sin \omega t \quad x(\tau_0) = x_0 \qquad (D.3)$$

Define the mapping $T : C(D_\beta,\Delta_\beta) \to C(D_\beta,\Delta_\beta)$

$$T[F](x_0,\tau_0) := \int_{-\infty}^{0} e^{\frac{s}{\beta}} K[s+\tau_0,x^F(s+\tau_0),F(s+\tau_0,x^F(s+\tau_0),\varepsilon,\beta),\beta]ds$$

where

$$K(\tau,x,F,\beta) := \cos x[\alpha - \sin x + \varepsilon \sin \omega\tau + F] - \varepsilon\omega \cos \omega\tau$$

Applying similar procedure to that of the proof of theorem 3.1 Bạris, and Fodchuk [3] has shown that for β sufficiently small, i.e., for β satisfying inequalities:

$$\beta(2 + \alpha + \varepsilon + \varepsilon\omega) \leq D_\beta$$
$$\beta(2 + \alpha + \varepsilon)(1 + \Delta_\beta) \leq \Delta_\beta$$
$$\beta(2 + \alpha + \varepsilon) < 1$$

Equations (3.1) possess an integral manifold S_β as defined in (3.16). Moreover this manifold is smooth and stable.

List of Figure Captions

Fig. 1. A second order Josephson junction circuit model driven by a dc and ac current source.

Fig. 2. Phase protraits of (2.1) for various values of α and β:

(a) $\alpha > 1$; (b) $\alpha = 1$, $\beta > \beta_0(1)$; (c) $0 < \alpha < 1$, $\beta > \beta_0(\alpha)$;

(d) $\alpha = 1$, $\beta = \beta_0(1)$; (e) $0 < \alpha < 1$, $\beta = \beta_0(\alpha)$ (f) $\alpha = 1$, $\beta < \beta_0(1)$;

(g) $0 < \alpha < 1$, $\beta < \beta_0(\alpha)$

Fig. 3. (a) The function $\alpha_0(\beta)$ is defined for all $\beta > 0$. On the α-β plane the region above $\alpha = 1$ corresponds to the phase portrait shown in Fig. 2(a), the region below the $\alpha = \alpha_0(\beta)$ characteristic corresponds to Fig. 2(g), the region $\alpha_0(\beta) < \alpha < 1$ corresponds to Fig. 2(c); the regions $\alpha = \alpha_0(\beta) = 1$; $\alpha = \alpha_0(\beta) < 1$; and $\alpha = 1$, $\beta > \beta_0(1)$ correspond to the portraits 2(f), 2(e), and 2(b) respectively; the point $\alpha = 1$, $\beta = \beta_0(1)$ corresponds to the portrait in Fig. 2(d).

(b) Qualitative relationship between critical current I_0 and capacitance C with other parameters held fixed. Here C_0 correponds to $\beta_0(1)$.

Fig. 4. Integral manifold S_0 of (2.1) represented by:

(a) a periodic surface in (τ,x,y)-space,

(b) a cylinder with the lines $x = k2\pi$, $k = 0,\pm1,\pm2,\ldots$ identified,

(c) a toroid with the lines $x = k2\pi$ and $\tau = \ell T$, $k,\ell = 0,\pm1,\pm2,\ldots$ identified.

Fig. 5. $I_{dc} - V_{dc}$ characteristic for β "large" and $\beta \leq \beta_0(1)$. For $|I_0| < |I_{dc}| \leq |I_c|$ the characteristic is double valued. $|V_{dc}|$ increases with $|I_{dc}|$ (i.e. with α) and also with β (for α fixed).

Fig. 6. Values of parameters ε, β for which integral manifold exists

(a) $\alpha \leq 1$, (b) $\alpha > 1$.

Fig. 7. For each point with coordinates (x_0,y_0) near the curve $y = \psi(x)$ there exists a unique pair (θ_0,ρ_0) and vice-versa, having the geometrical relationship indicated. Note that θ_0 is equal numerically to the x-coordinate of the intersection point $\hat{P}_0$, and ρ_0 is just the vertical distance from P_0 to $\hat{P}_0$.

Fig. 8. Integral manifolds for (3.1) for small ε:

(a) for $\alpha > 1$ the steady state solution lies on a 2-dimensional surface S_ε

(b) for $\alpha < 1$ and $\alpha < \alpha_0(\beta)$ a steady state (periodic) solution exists in a neighborhood of each equilibrium point of (2.1).

Fig. 9. For small β and $\alpha < \alpha_0(\beta_0)$ only the integral manifold S_β exists.

Fig. 10. The doubly-periodic surfaces S_ε and S_β in (a) can be represented as a cylinder in (b) or as a torus in (c).

Fig. 11. A bounded waveform which has no average.

Fig. 12. For any point P_0 on cross-section C (at τ_0) $\gamma(P_0) = P_1$ denotes the point where the trajectory from P_0 first intersects with C. Hence, $\gamma(P_1) = P_2$.

Fig. 13. (a) Poincaré map for $\dot{\phi} = \frac{\omega}{2}$. (b) Second iterated Poincaré map for $\dot{\phi} = \frac{\omega}{2}$.

Fig. 14. (a) Trajectories of $\dot{\phi} = \sin \phi$. (b) Poincaré map for $\dot{\phi} = \sin \phi$.

Fig. 15. (a) A periodic trajectory on S_ε or S_β having rotation number $\mu = 3$ $(p = 3,\ q = 1)$.

(b) The corresponding trajectory on the torus.

Fig. 16. All trajectories of (4.17) are trapped within the horizontal strip $|\phi| \leq \frac{3\pi}{2}$.

Fig. 17. Step-wise discontinuous voltage phenomenon.

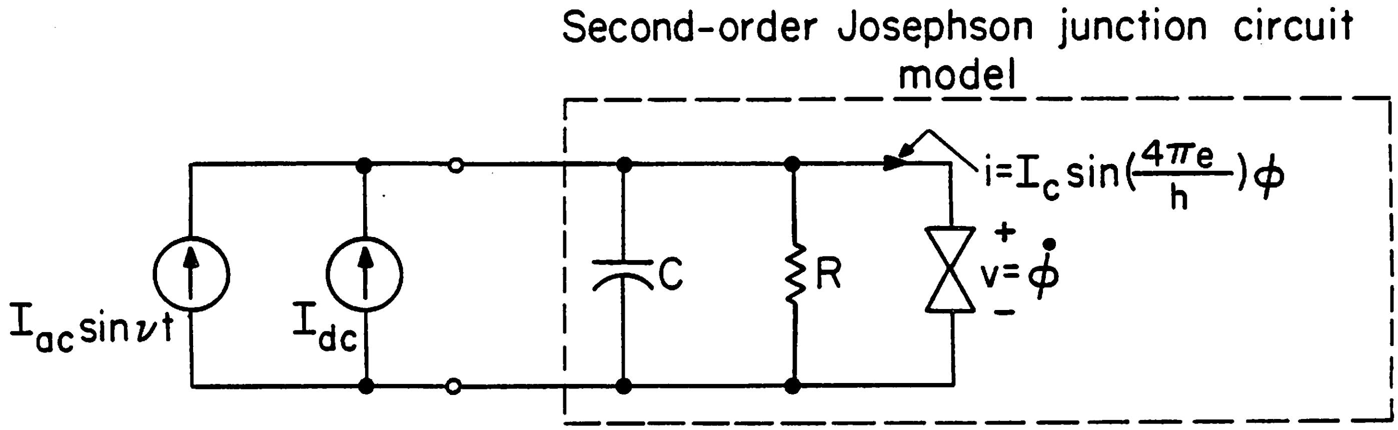

Fig. 1

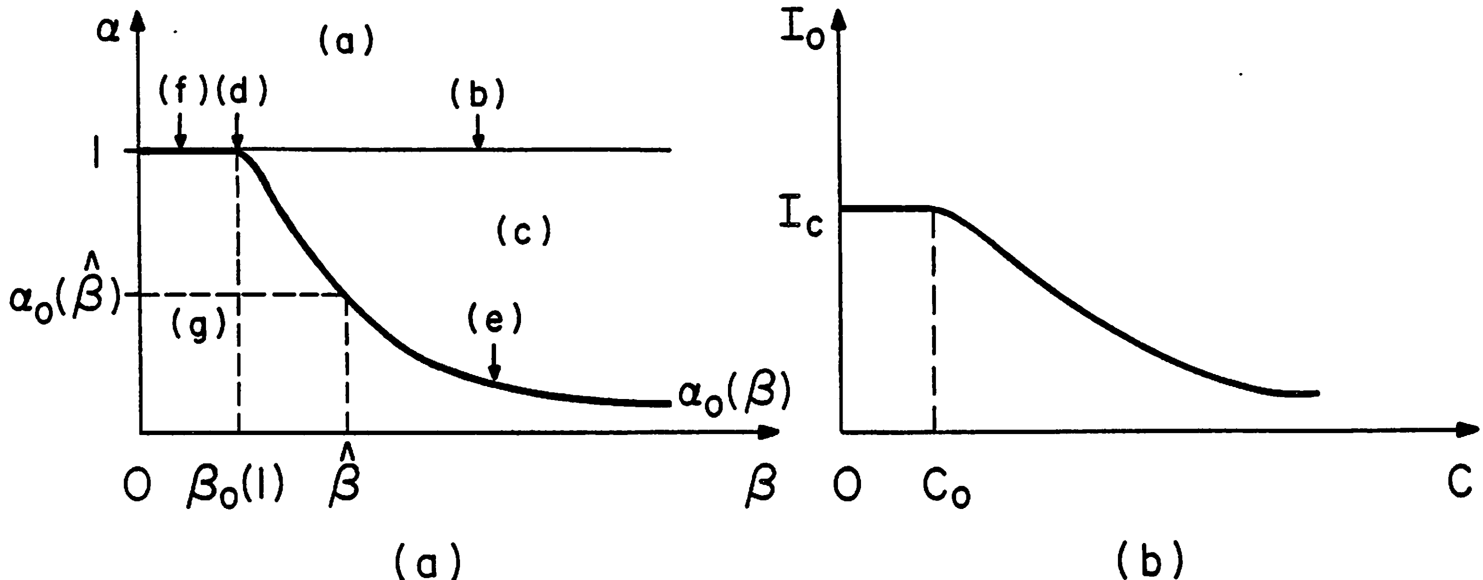

Fig. 3

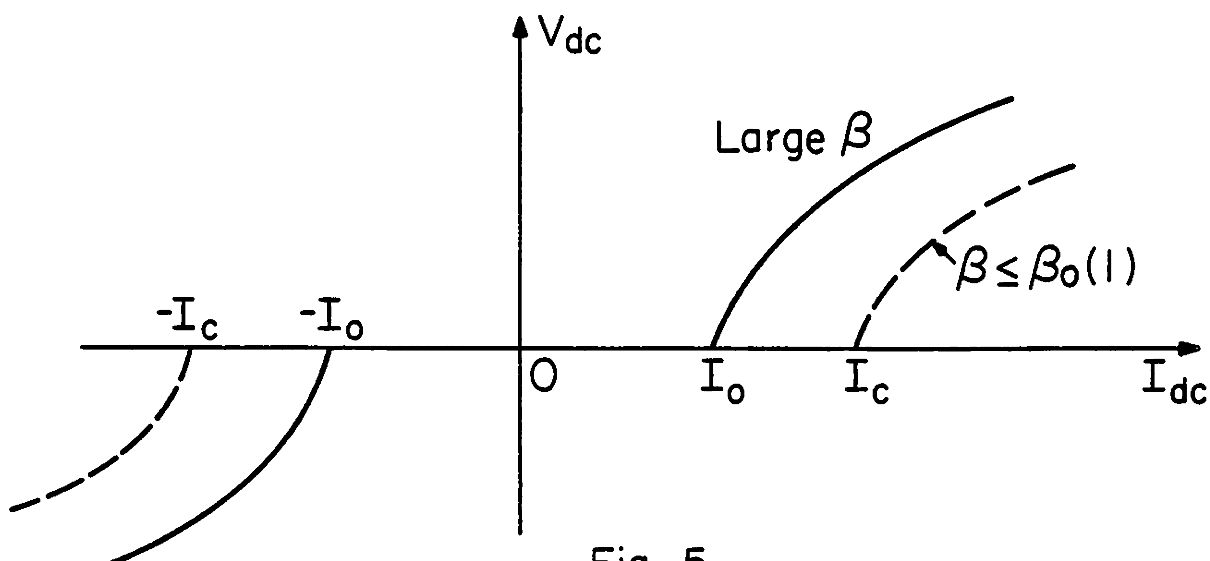

Fig. 5

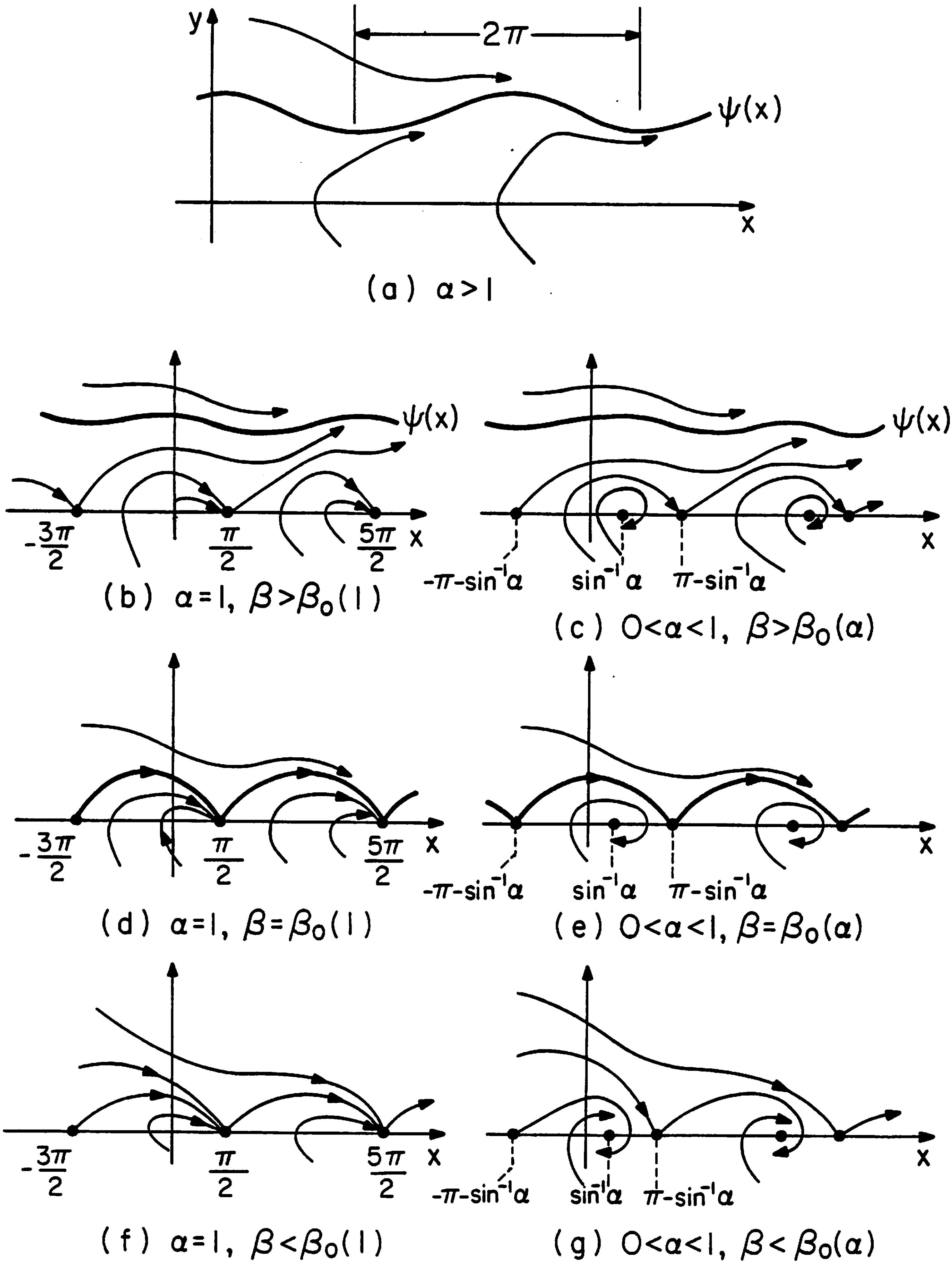

y
2π
ψ(x)
x
(a) α>1
ψ(x)
-3π/2
π/2
5π/2
x
(b) α=1, β>β0(1)
ψ(x)
x
-π-sin⁻¹α
sin⁻¹α
π-sin⁻¹α
(c) 0<α<1, β>β0(α)
-3π/2
π/2
5π/2
x
(d) α=1, β=β0(1)
x
-π-sin⁻¹α
sin⁻¹α
π-sin⁻¹α
(e) 0<α<1, β=β0(α)
-3π/2
π/2
5π/2
x
(f) α=1, β<β0(1)
x
-π-sin⁻¹α
sin⁻¹α
π-sin⁻¹α
(g) 0<α<1, β<β0(α)

Fig. 2

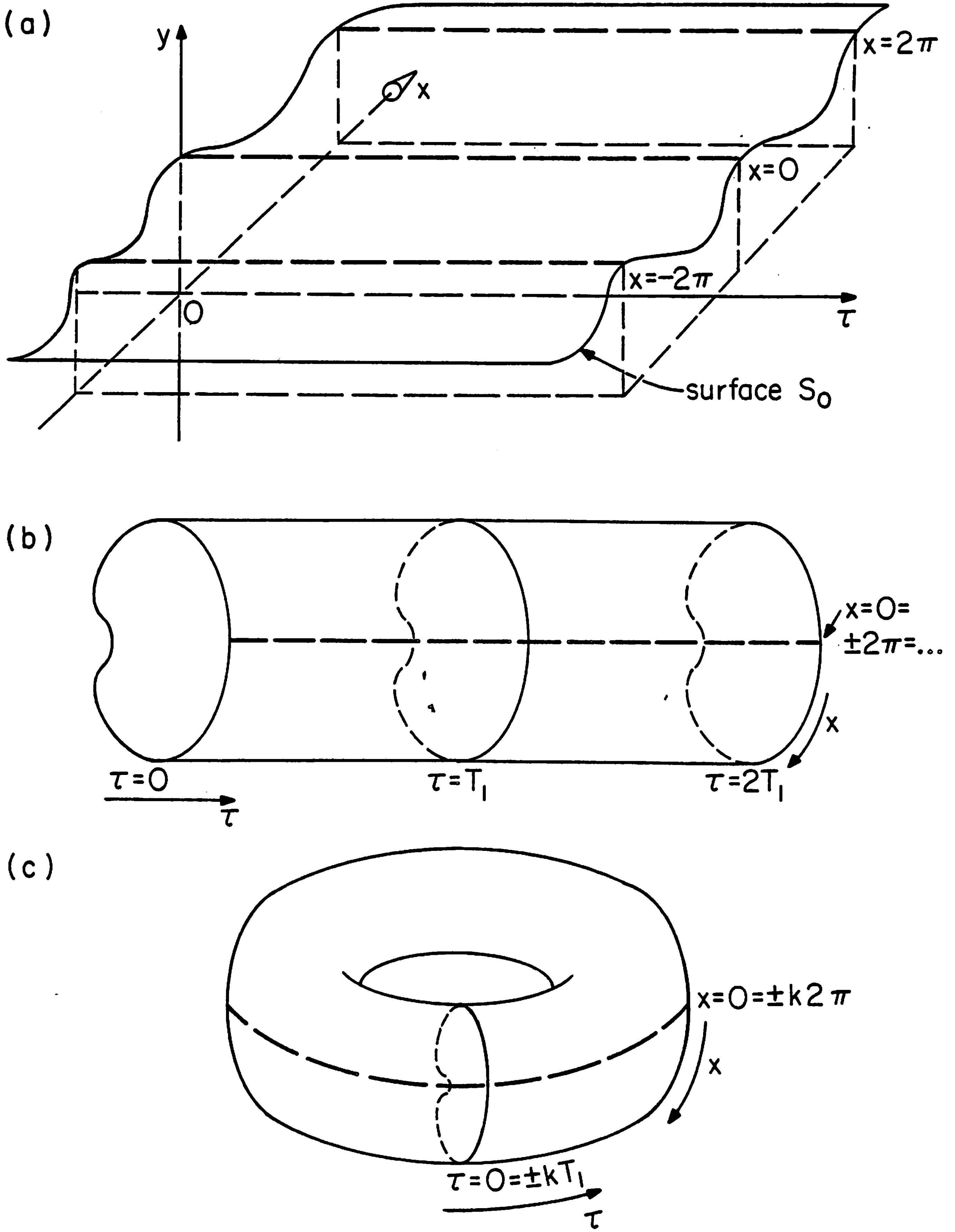
(a)
y
x
x=2π
x=0
x=−2π
O
τ
surface S_0
(b)
x=0=
±2π=...
x
τ=0
τ=T_1
τ=2T_1
τ
(c)
x=0=±k2π
x
τ=0=±kT_1
τ

Fig. 4

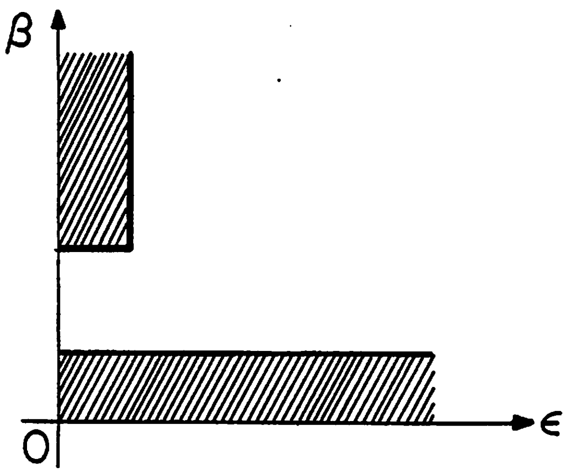
β
O
ε
(a) α ≤ 1

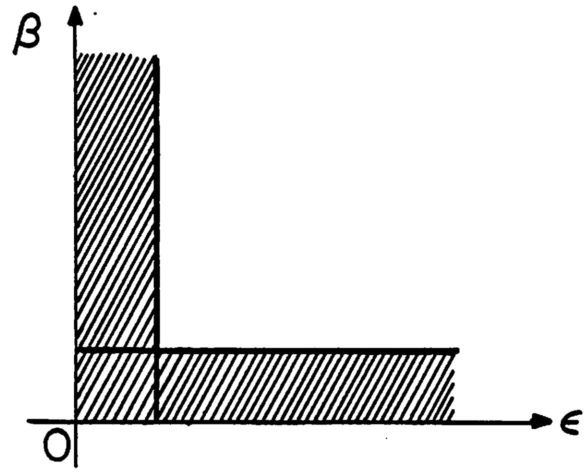
β
O
ε
(b) α > 1

Fig. 6

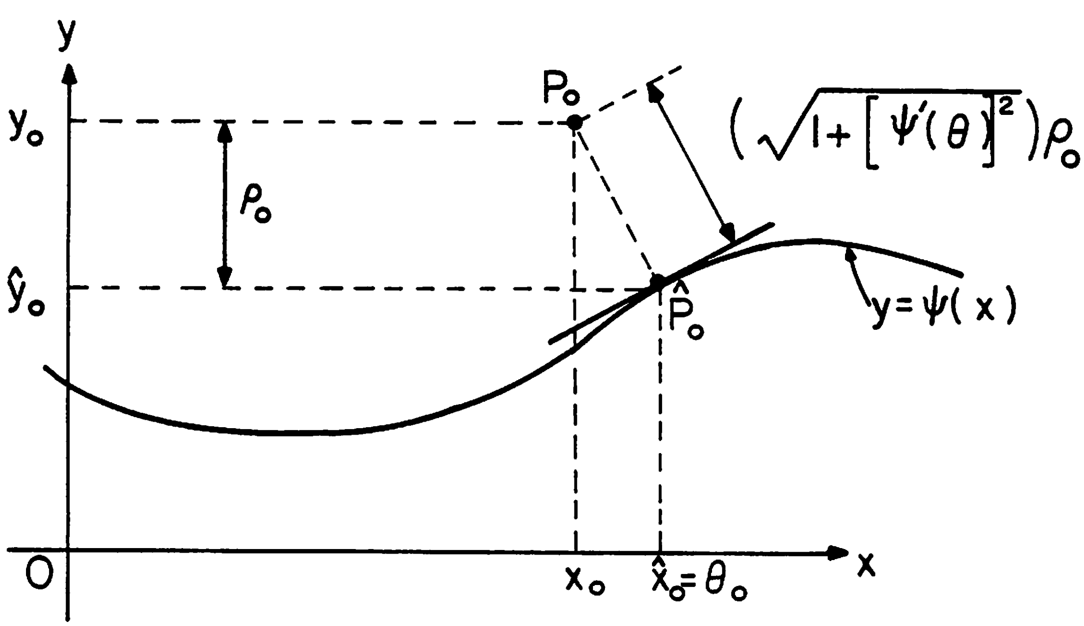
y
y_o
$\hat{y}_o$
ρ_o
P_o
$\hat{P}_o$
$\left(\sqrt{1+[\psi'(\theta)]^2}\right)\rho_o$
$y=\psi(x)$
O
x_o
$\hat{x}_o=\theta_o$
x

Fig. 7

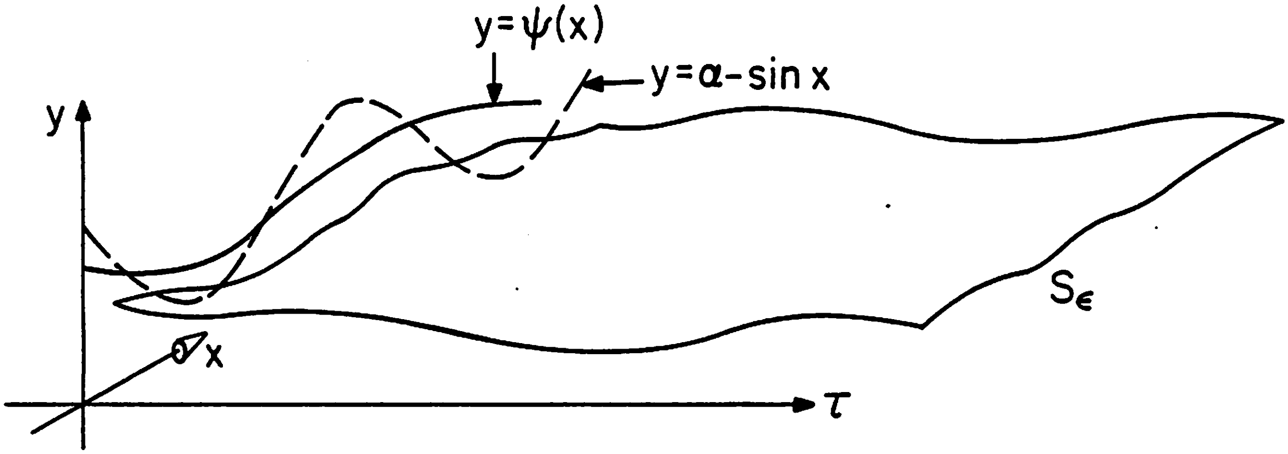

(a) α>1
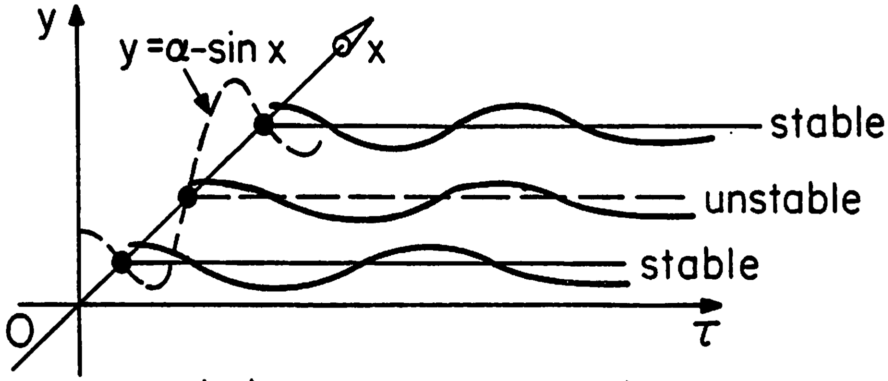

(b) α<1 and α<α₀(β)

Fig. 8

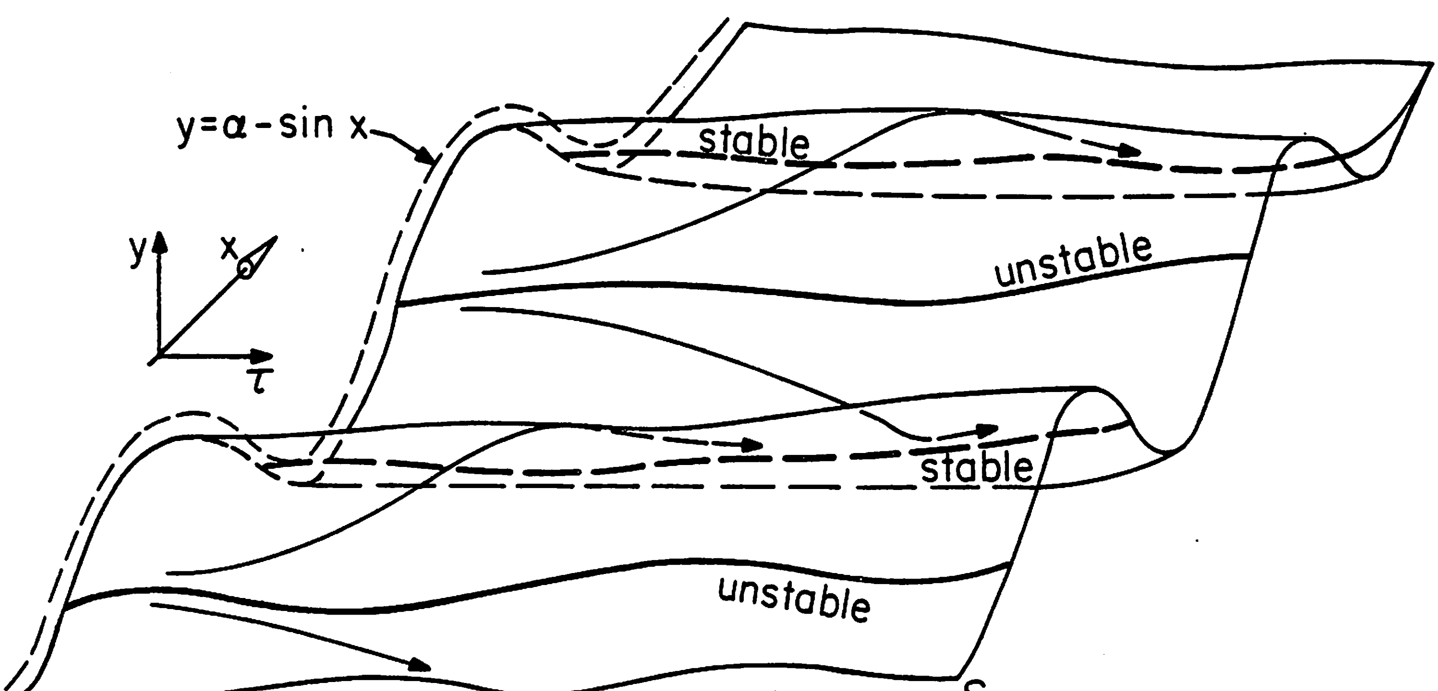

Fig. 9

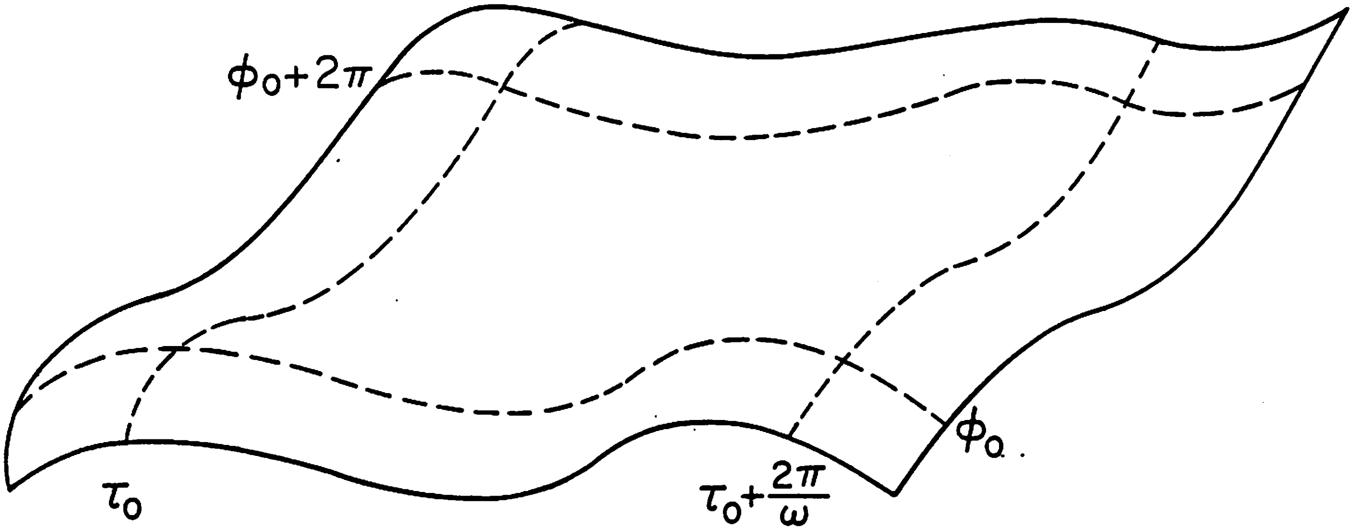

$\phi_0 + 2\pi$
ϕ_0
τ_0
$\tau_0 + \frac{2\pi}{\omega}$

(a)

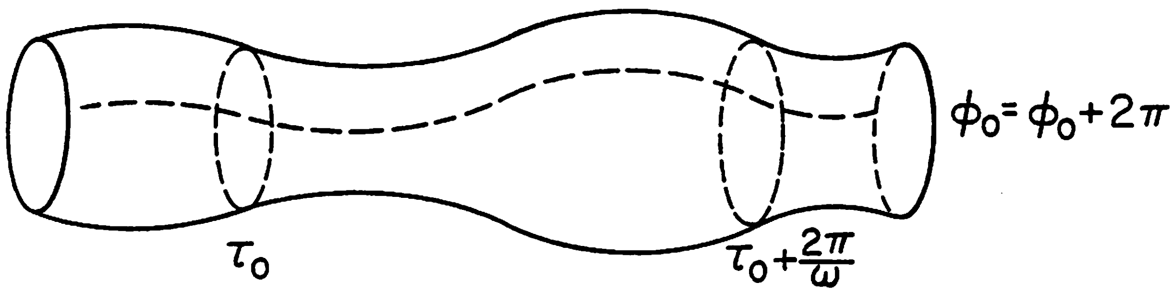

$\phi_0 = \phi_0 + 2\pi$
τ_0
$\tau_0 + \frac{2\pi}{\omega}$

(b)

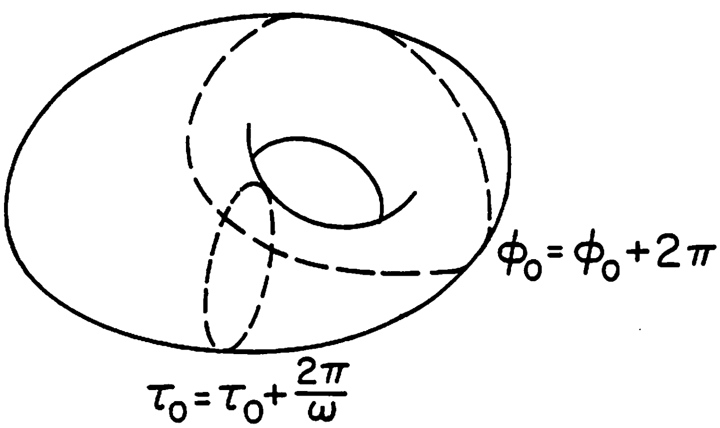

$\phi_0 = \phi_0 + 2\pi$
$\tau_0 = \tau_0 + \frac{2\pi}{\omega}$

(c)

Fig. 10

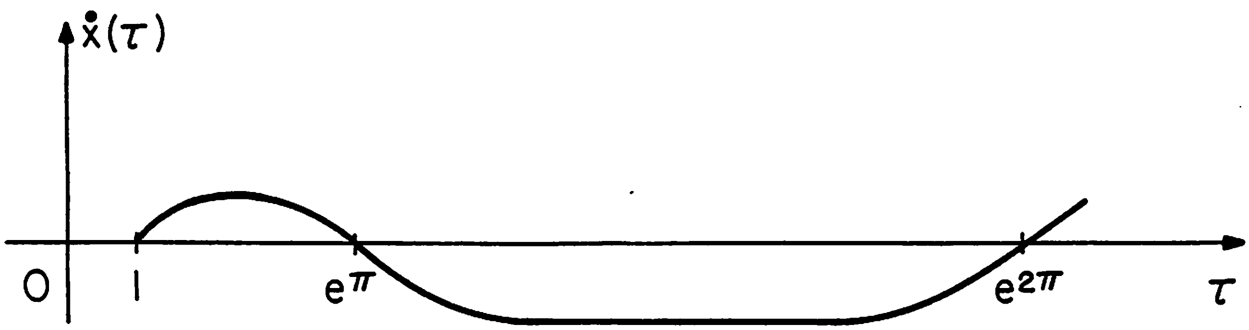

Fig. 11

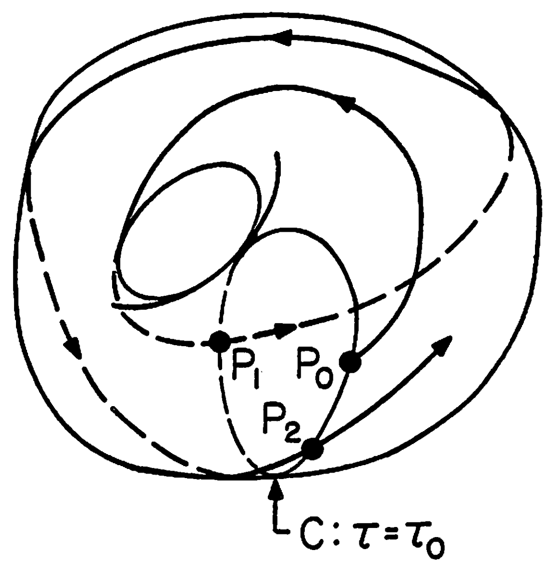

Fig. 12

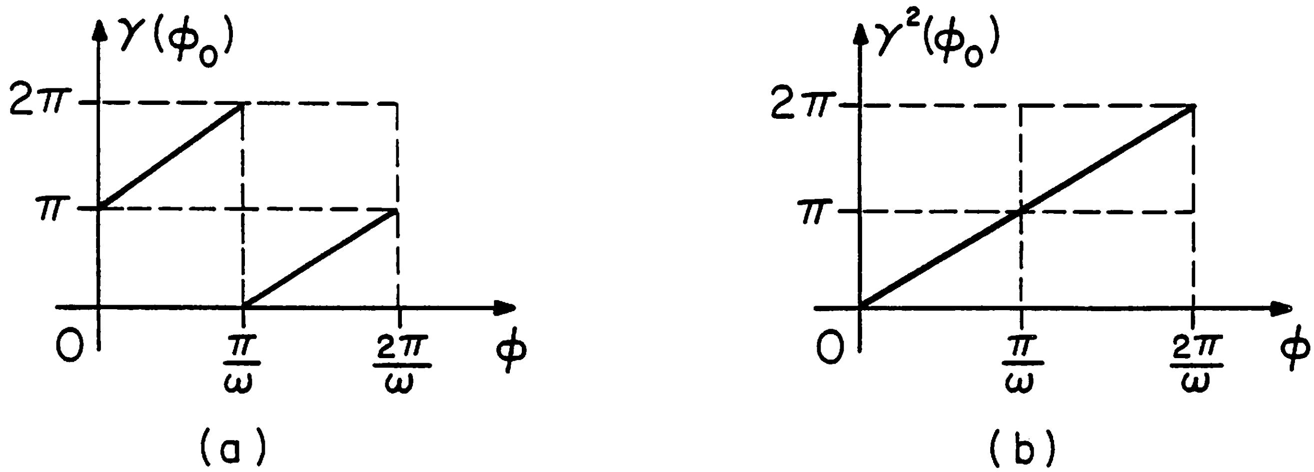

Fig. 13

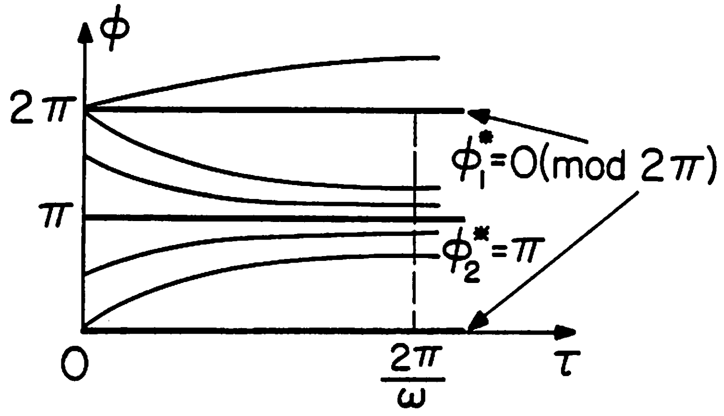

(a)

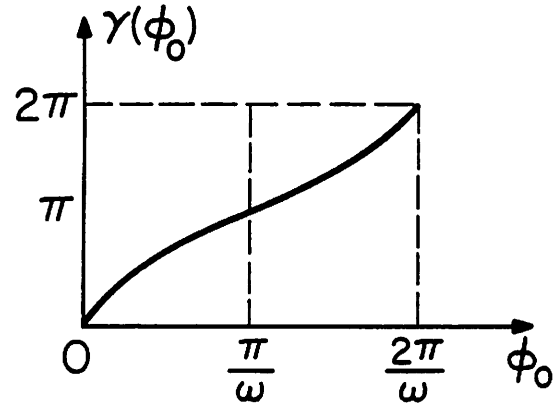

(b)

Fig. 14

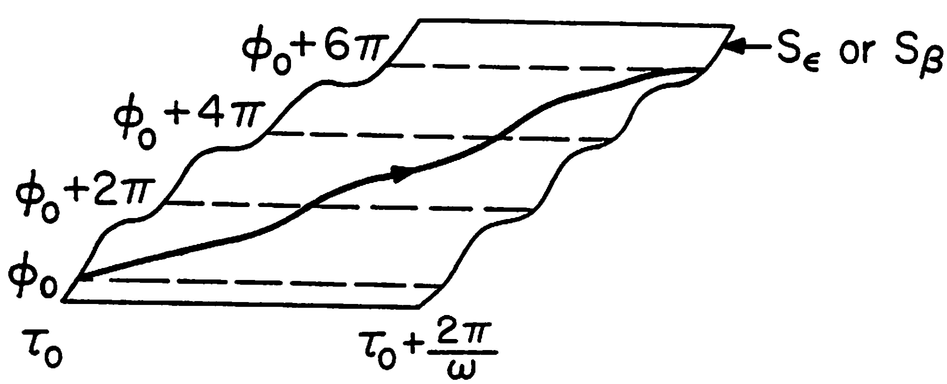

(a)

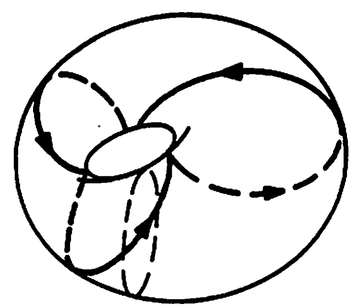

(b)

Fig. 15

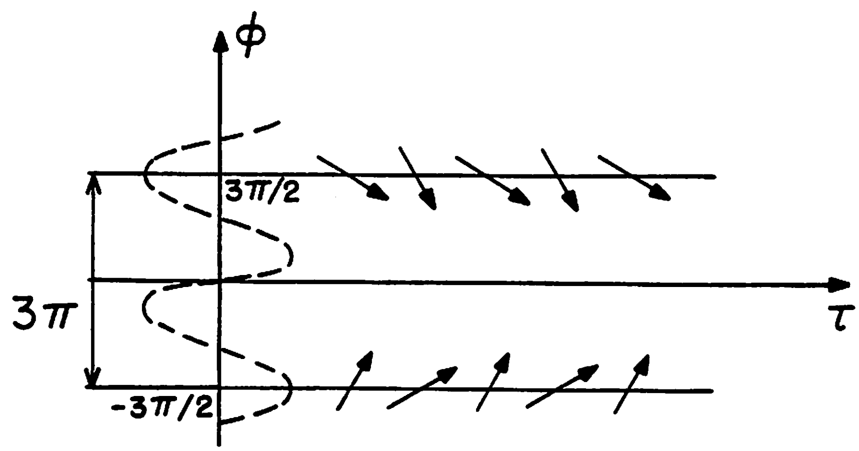

Fig. 16

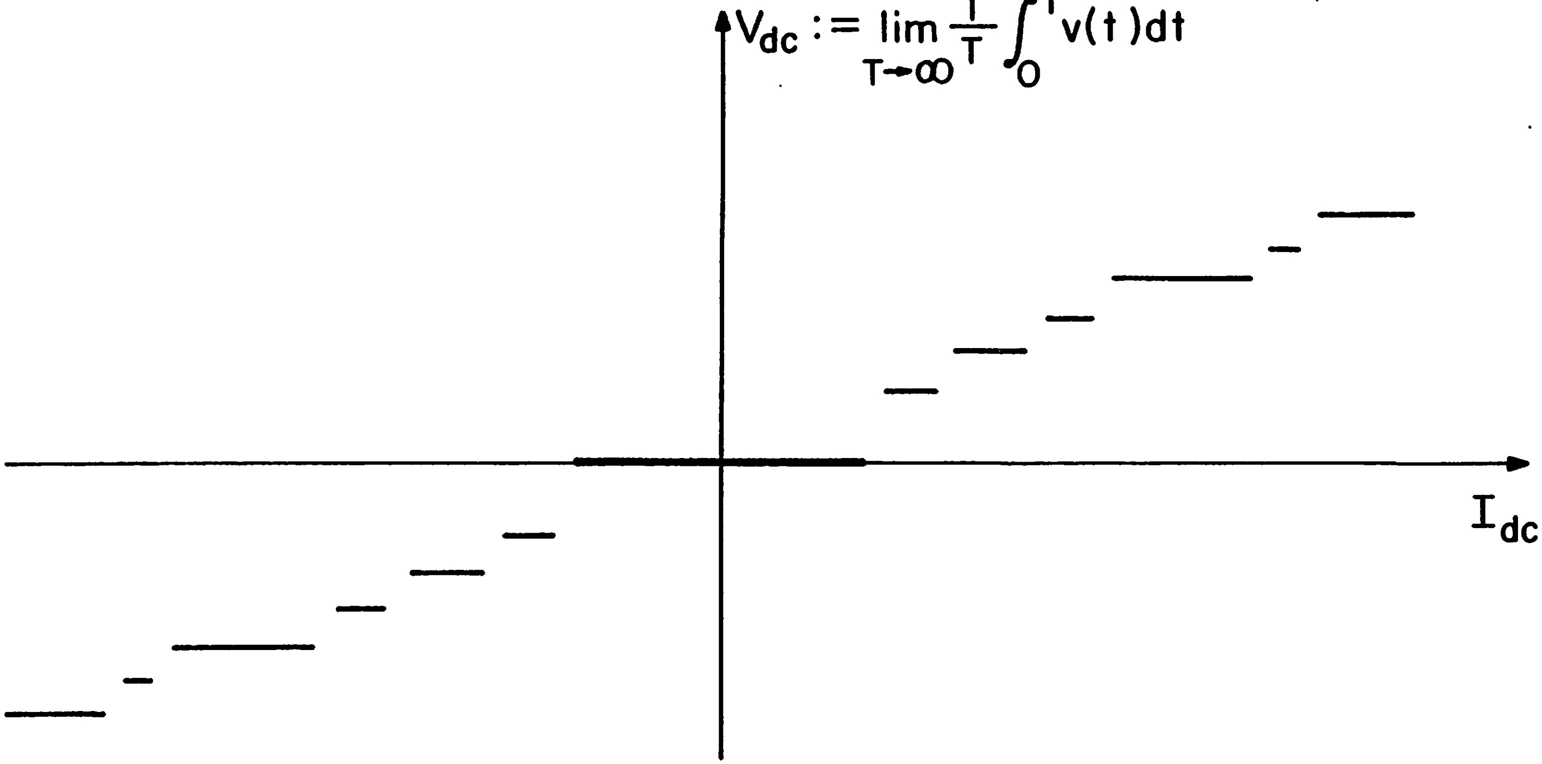

Fig. 17

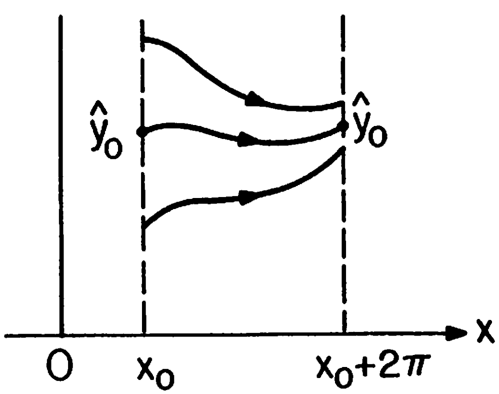

Fig. A1

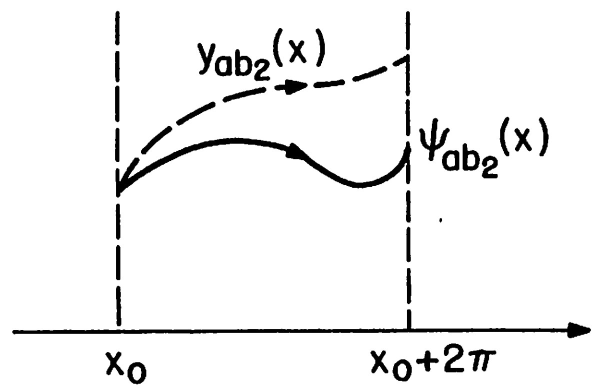

Fig. A3

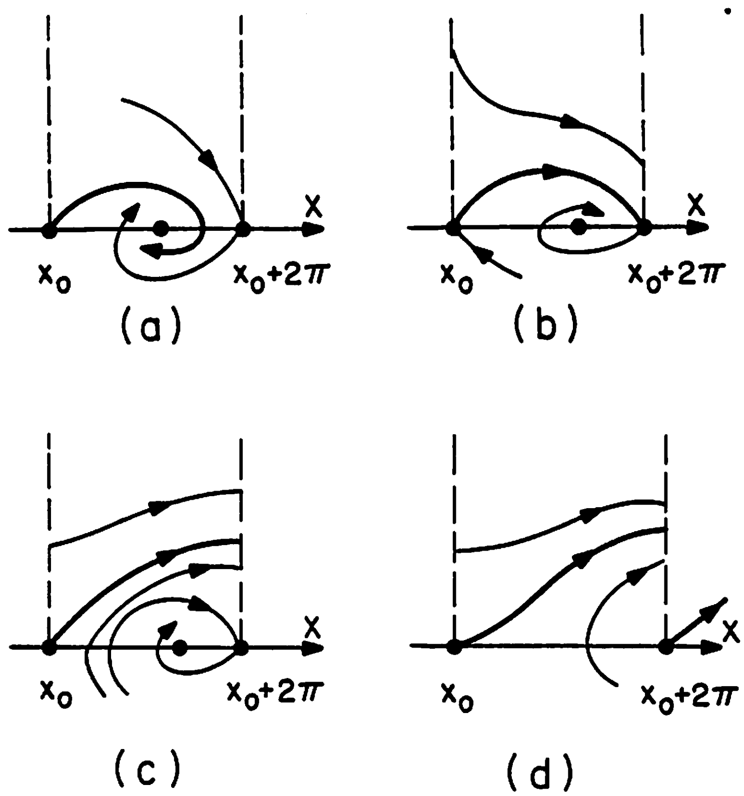
X
x_0
$x_0+2\pi$
(a)
X
x_0
$x_0+2\pi$
(b)
X
x_0
$x_0+2\pi$
(c)
X
x_0
$x_0+2\pi$
(d)

Fig. A2

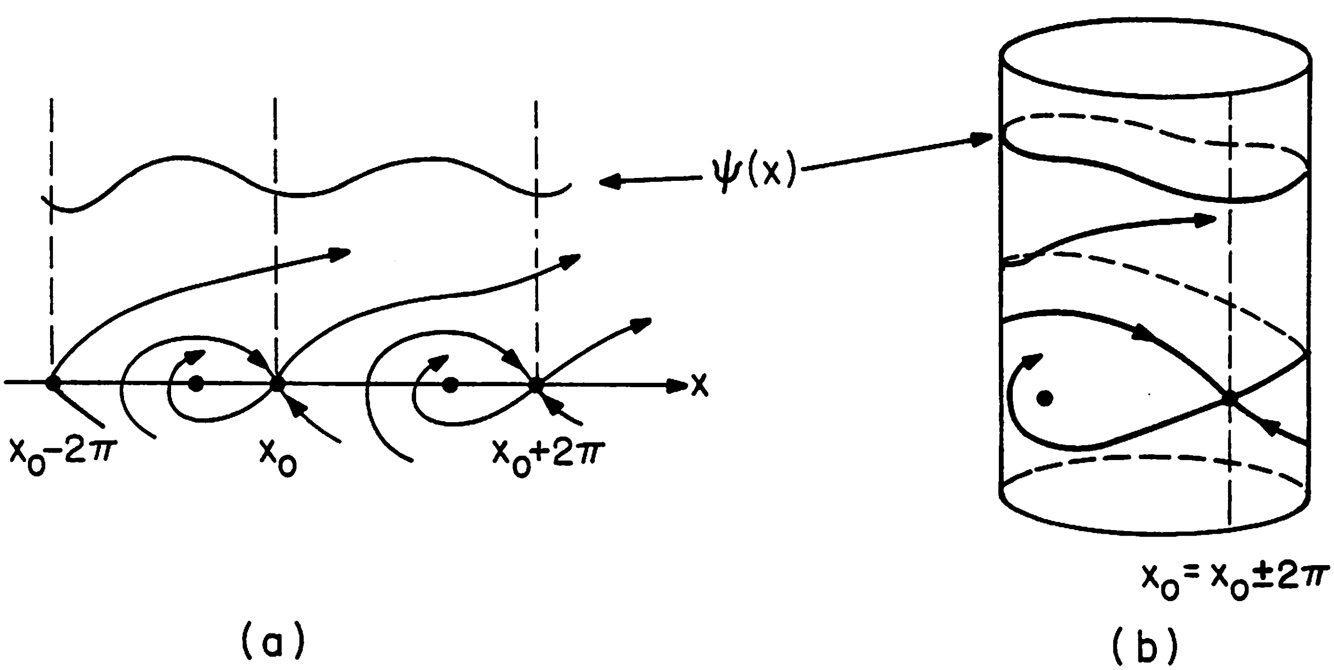
$\psi(x)$
X
$x_0-2\pi$
x_0
$x_0+2\pi$
$x_0=x_0\pm2\pi$
(a)
(b)

Fig. A4